Supporting Information I

Bismuth(III)dichalcogenones: Highly Active Catalysts in Multiple C–C Bond Formation Reactions

Katam Srinivas, Arruri Sathyanarayana, Chatla Naga Babu and Ganesan Prabusankar*

Department of Chemistry, Indian Institute of Technology Hyderabad, Kandi,

Medak, TS, INDIA-502 285.

Fax: +91 40 2301 6032; Tel: +91 40 2301 6089; E-mail: prabu@iith.ac.in

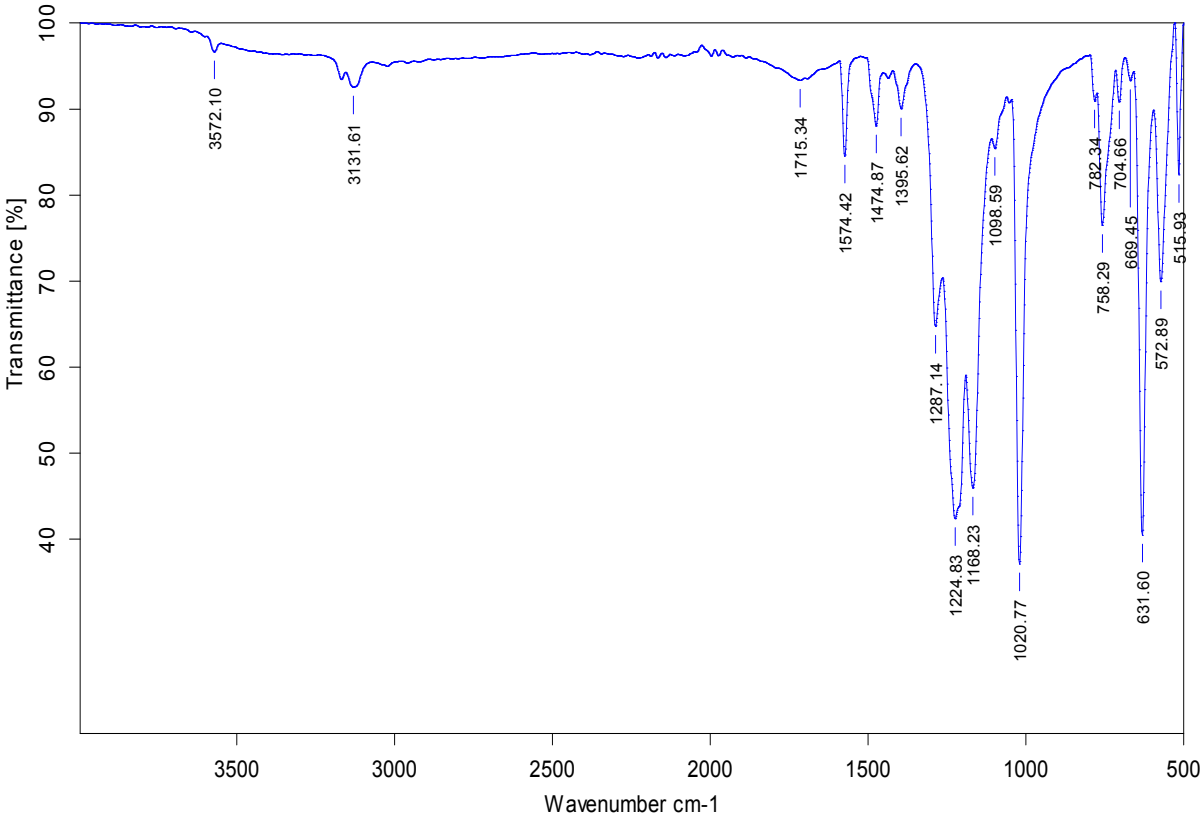

Fig. S1. Neat FT-IR spectrum of $[(mbit)_3Bi](OTf)[Bi_6(OTf)_{12}(\mu_3\text{-}OH)_8]$ (**1**).

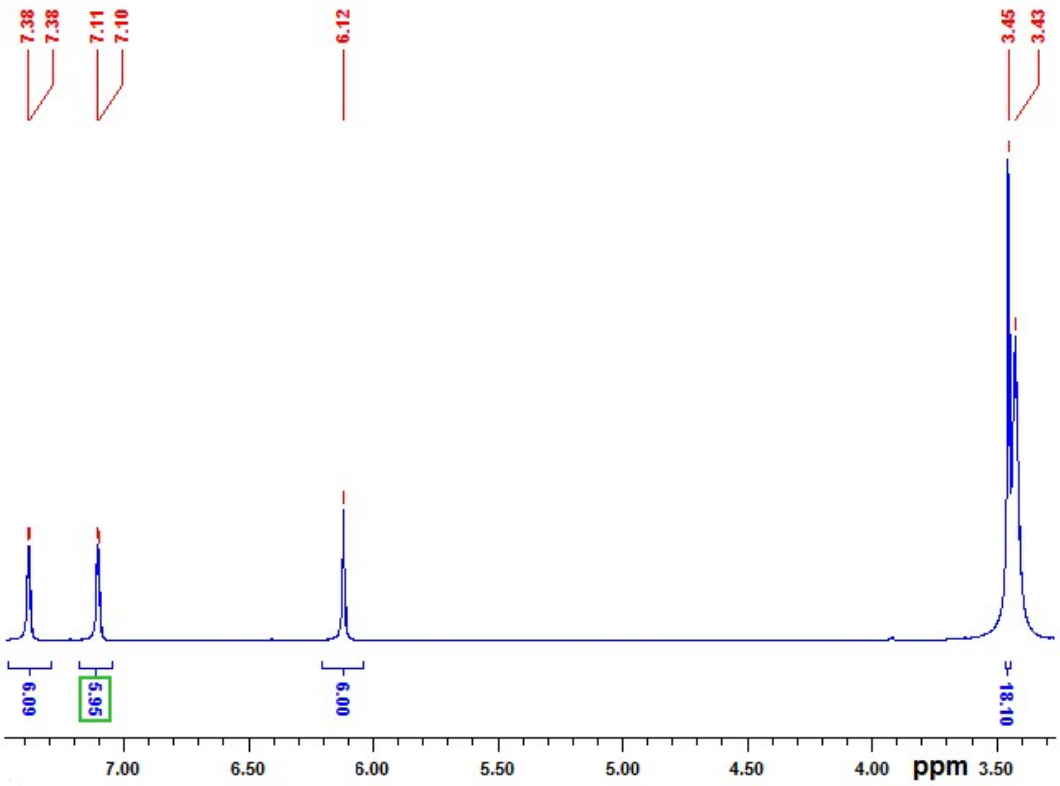

Fig. S2. ^{1}H NMR spectrum of $[(mbit)_3Bi](OTf)[Bi_6(OTf)_{12}(\mu_3\text{-}OH)_8]$ (**1**) in DMSO-d_6 at RT.

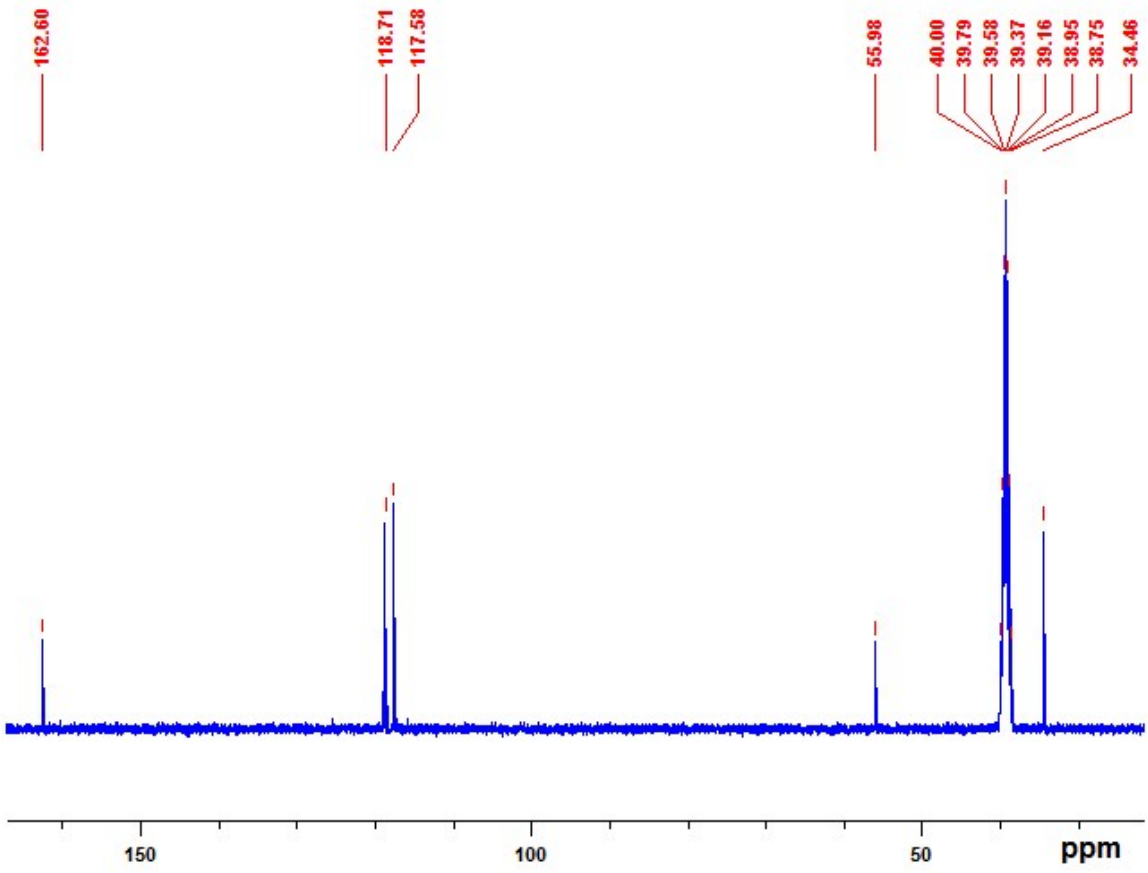

Fig. S3. ^{13}C NMR spectrum of [(mbit)$_3$Bi](OTf)[Bi$_6$(OTf)$_{12}$(μ_3-OH)$_8$] (**1**) in DMSO-d$_6$ at RT.

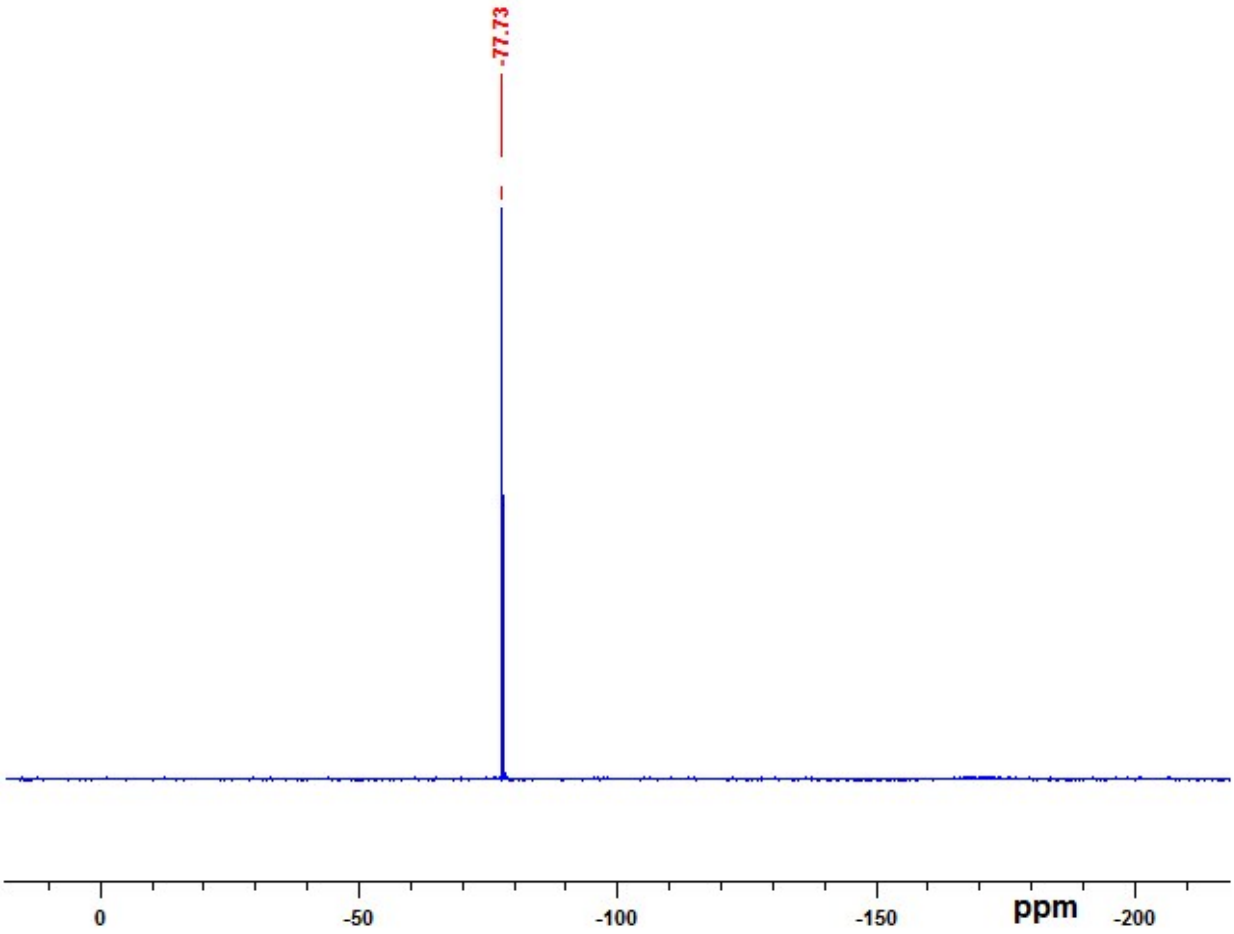

Fig. S4. ^{19}F NMR spectrum of $[(mbit)_3Bi](OTf)[Bi_6(OTf)_{12}(\mu_3\text{-}OH)_8]$ (**1**) in DMSO-d_6 at RT.

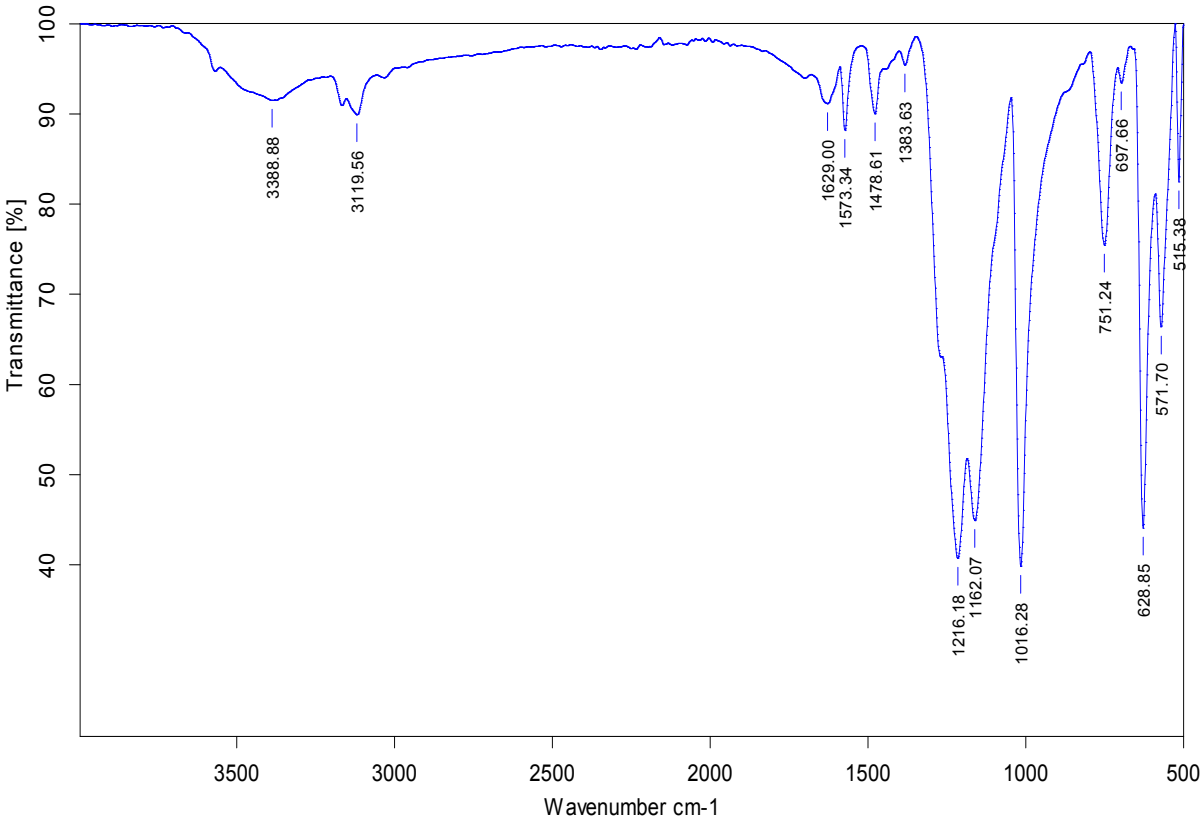

Fig. S5. Neat FT-IR spectrum of $[(mbis)_2(OTf)_2Bi](OTf).2CH_3OH$ (**2**).

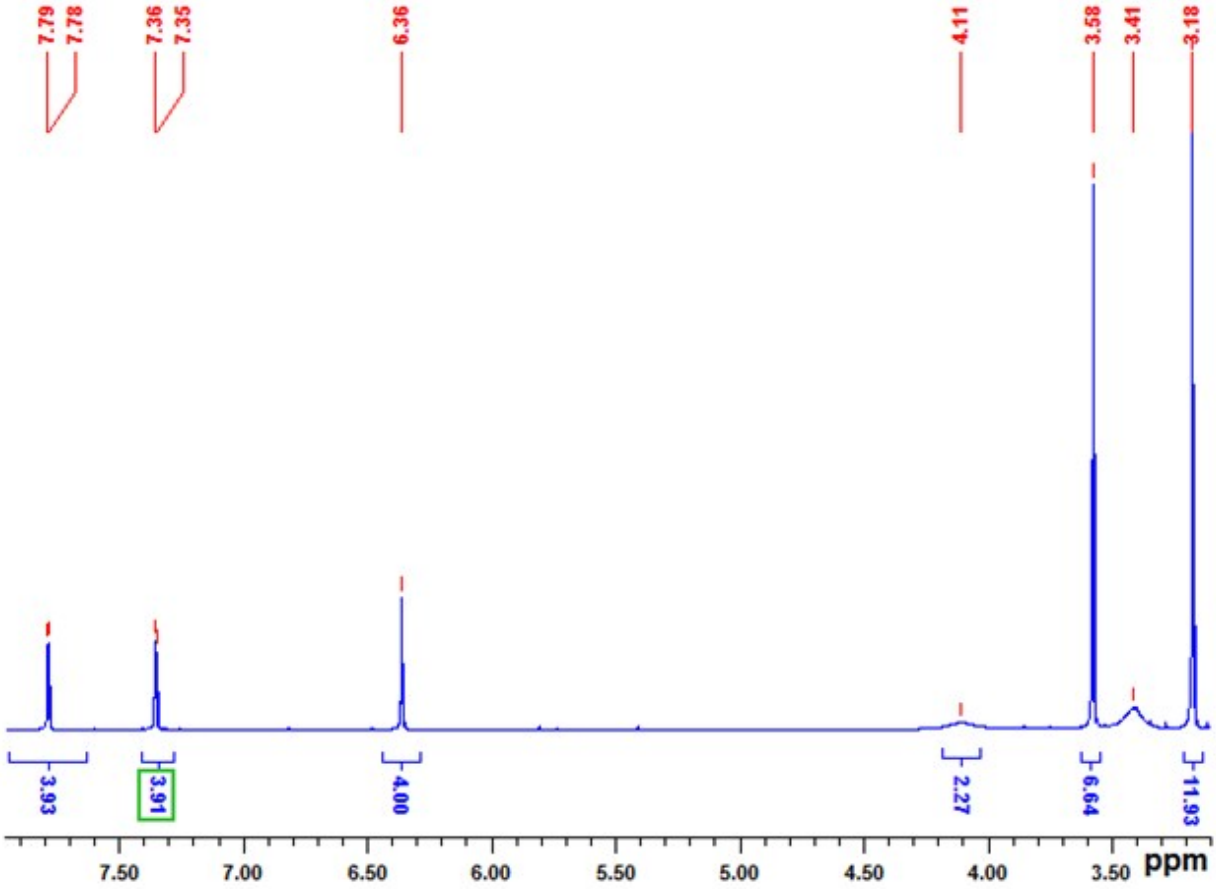

Fig. S6. ^{1}H NMR spectrum of $[(mbis)_2(OTf)_2Bi](OTf).2CH_3OH$ (**2**) in DMSO-d_6 at RT.

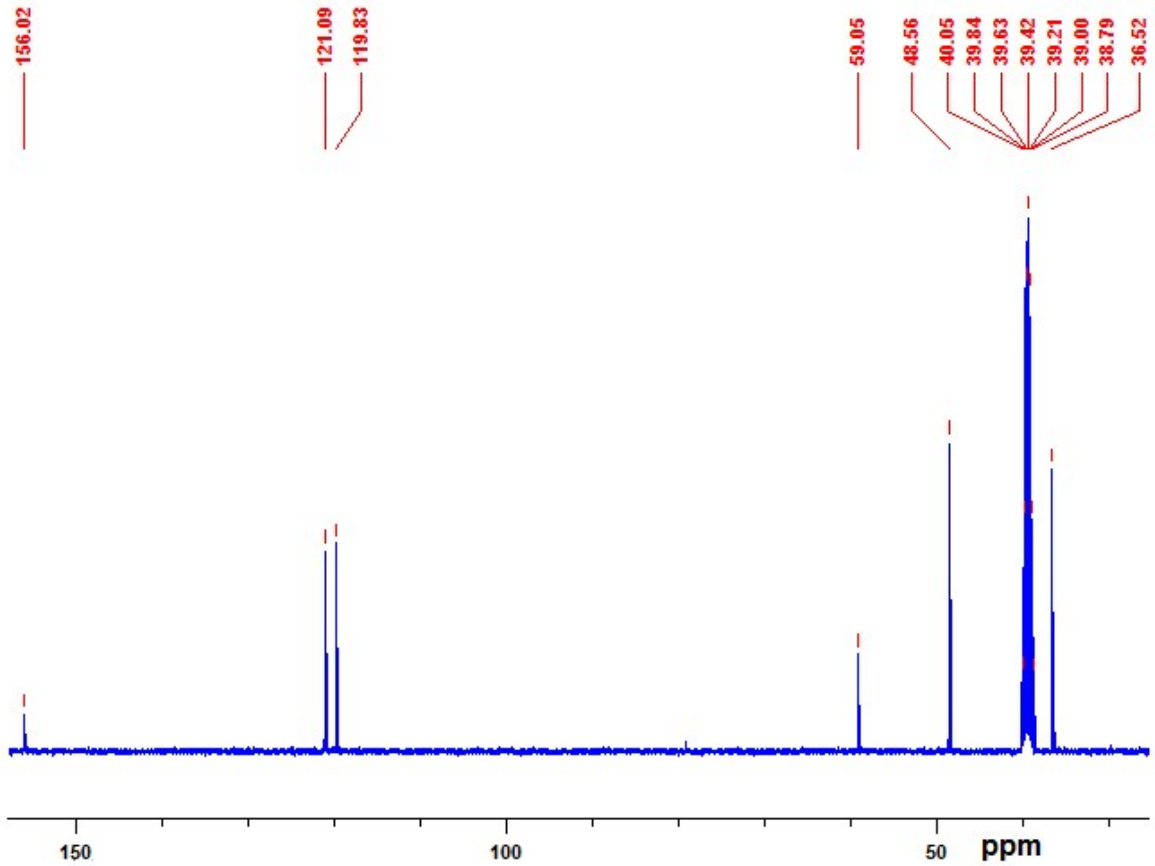

Fig. S7. ^{13}C NMR spectrum of $[(mbis)_2(OTf)_2Bi](OTf).2CH_3OH$ (**2**) in DMSO-d_6 at RT.

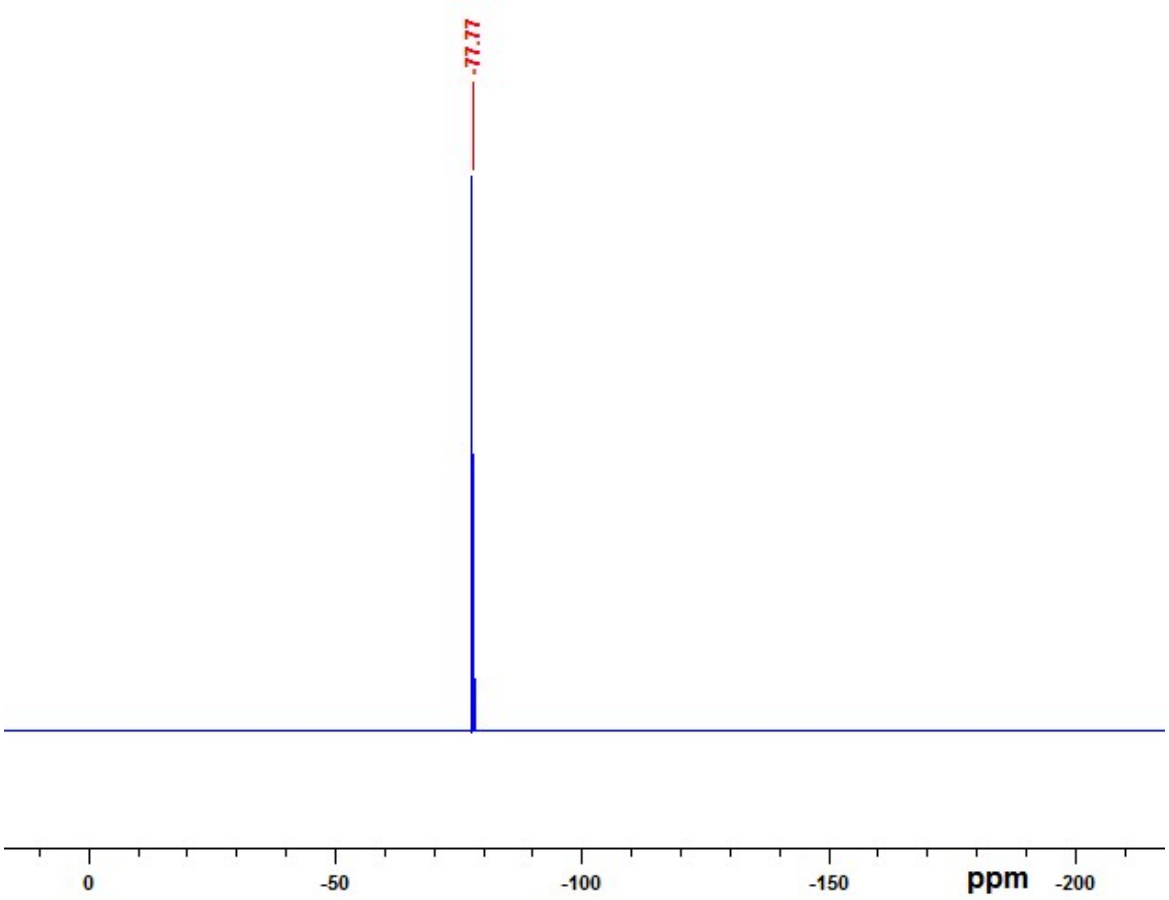

Fig. S8. ^{19}F NMR spectrum of $[(mbis)_2(OTf)_2Bi](OTf).2CH_3OH$ (**2**) in DMSO-d_6 at RT.

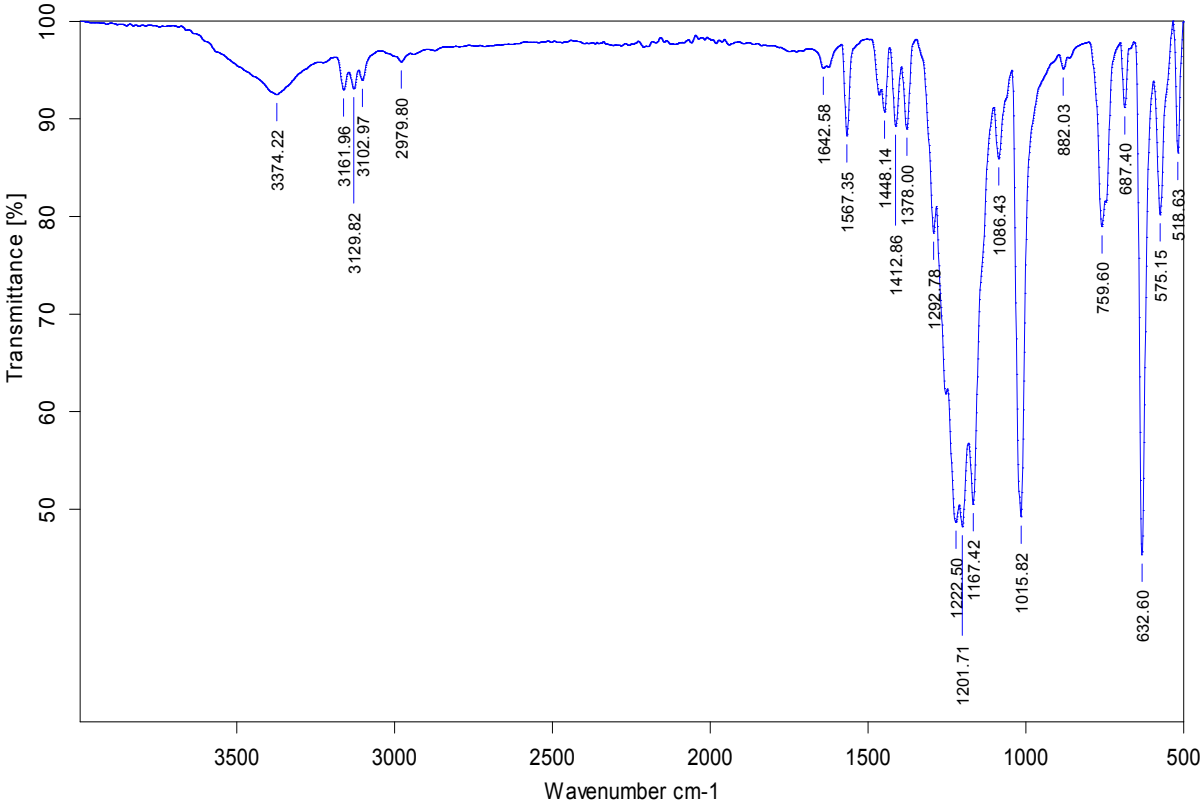

Fig. S9. Neat FT-IR spectrum of $[(mbpit)_2(OTf)_2Bi](OTf)$ (**3**).

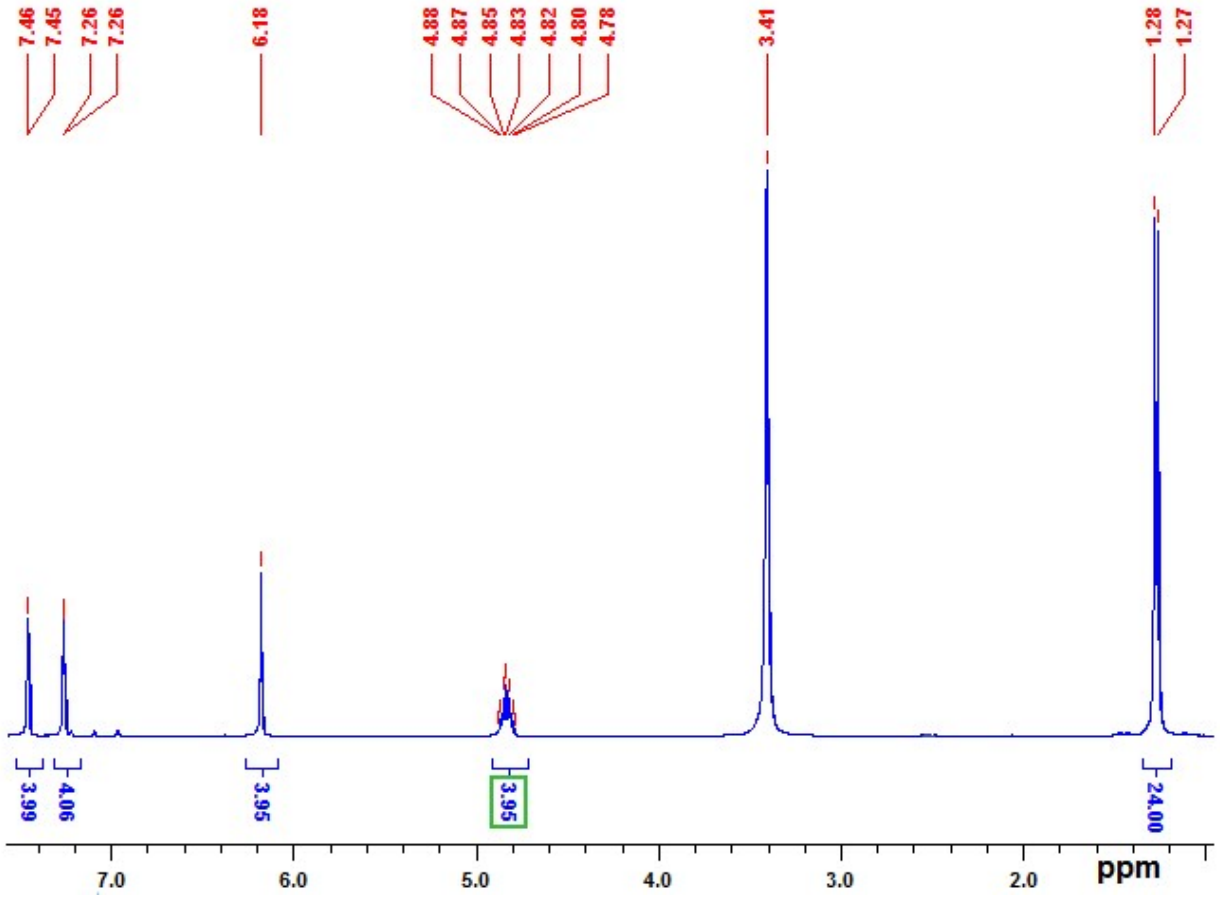

Fig. S10. ^{1}H NMR spectrum of [(mbpit)$_2$(OTf)$_2$Bi](OTf) (**3**) in DMSO-d$_6$ at RT.

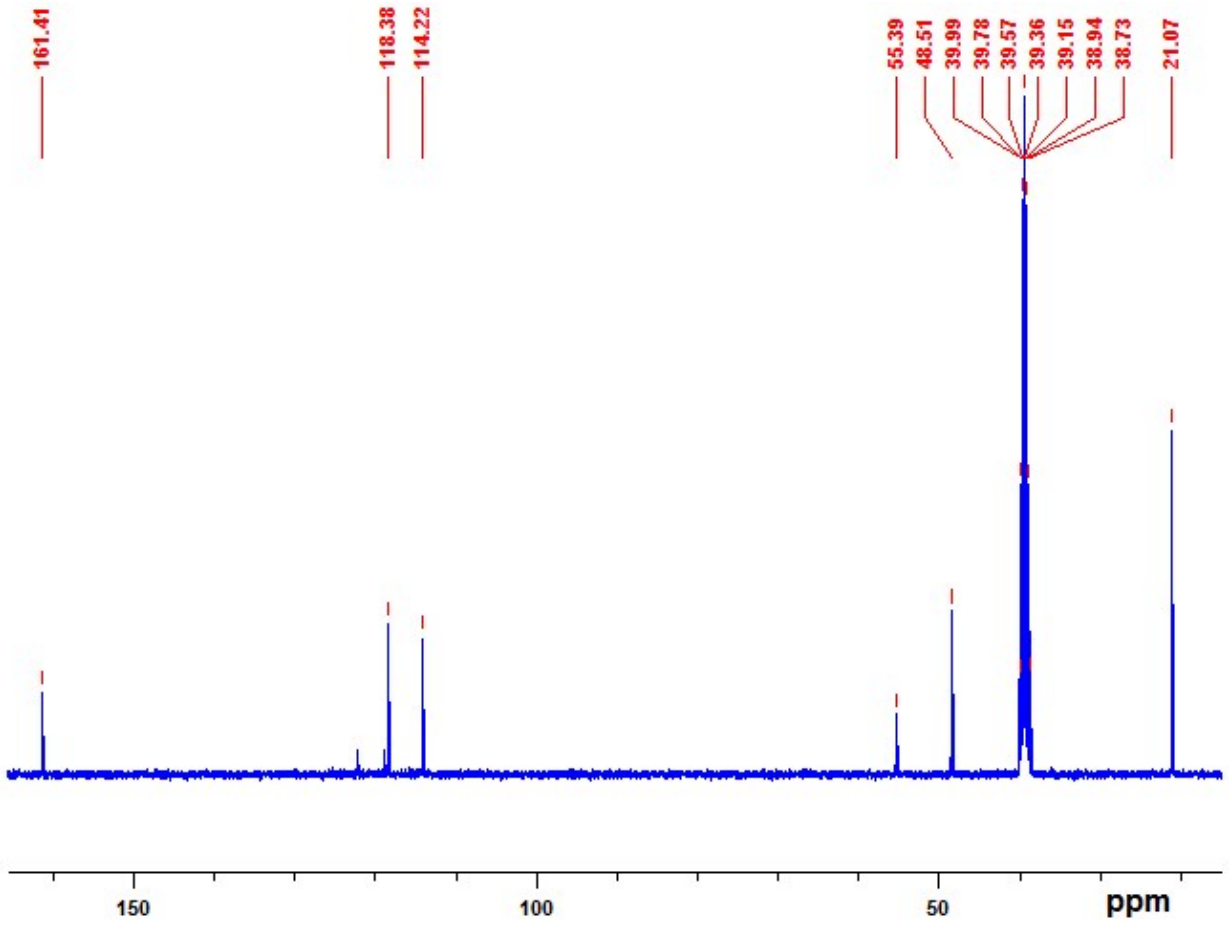

Fig. S11. ^{13}C NMR spectrum of $[(mbpit)_2(OTf)_2Bi](OTf)$ (**3**) in DMSO-d_6 at RT.

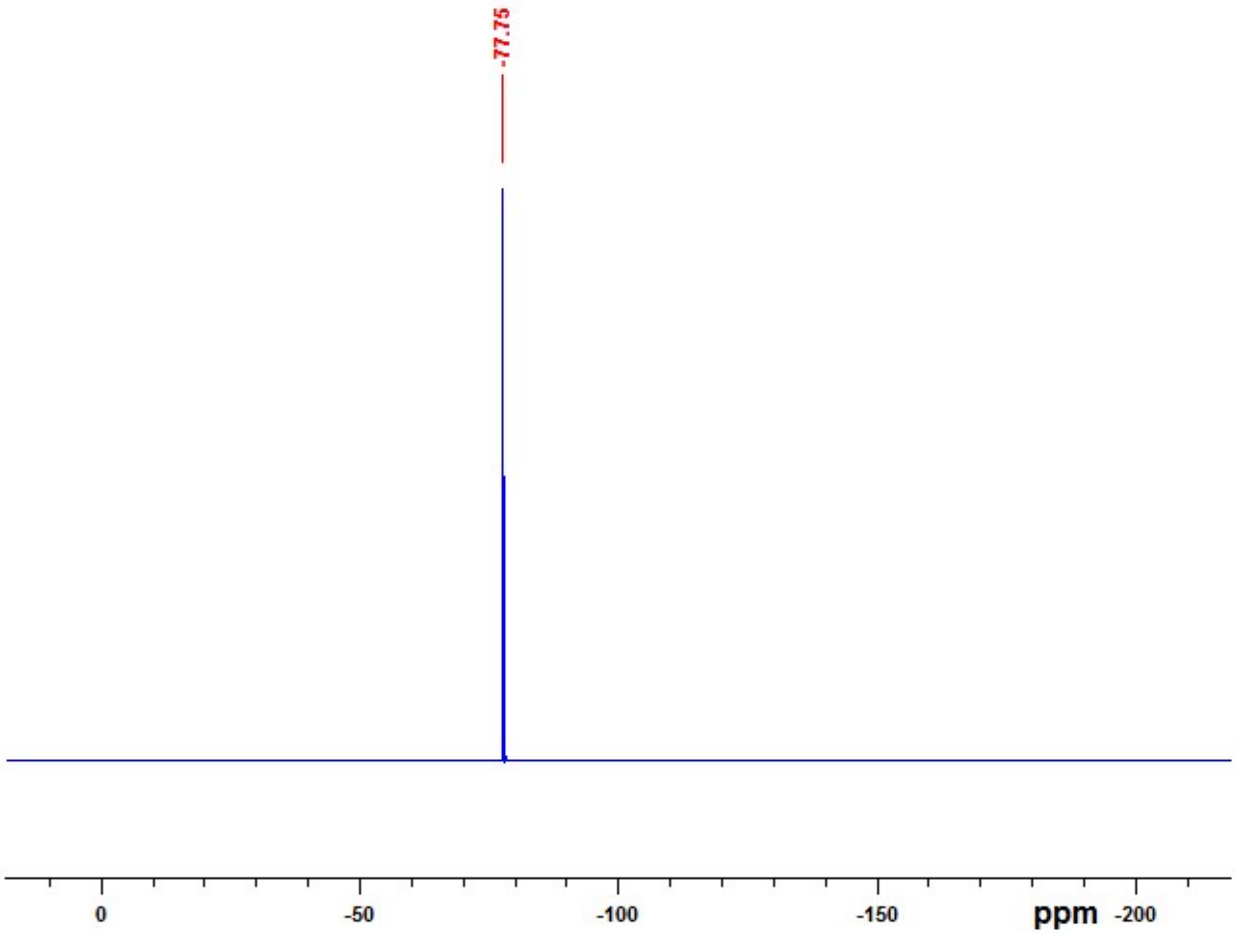

Fig. S12. ^{19}F NMR spectrum of $[(mbpit)_2(OTf)_2Bi](OTf)$ (**3**) in DMSO-d_6 at RT.

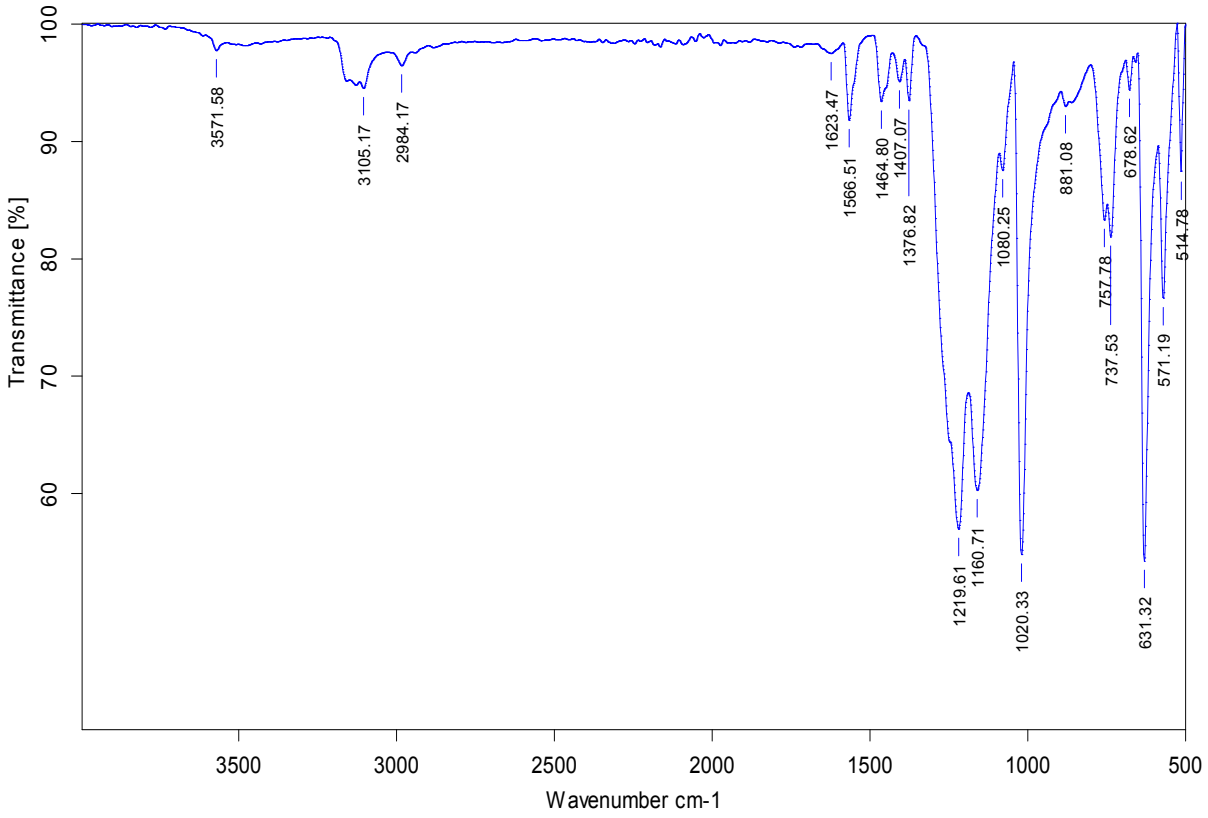

Fig. S13. Neat FT-IR spectrum of $[(mbpis)_2(OTf)_2Bi](OTf)$ (**4**).

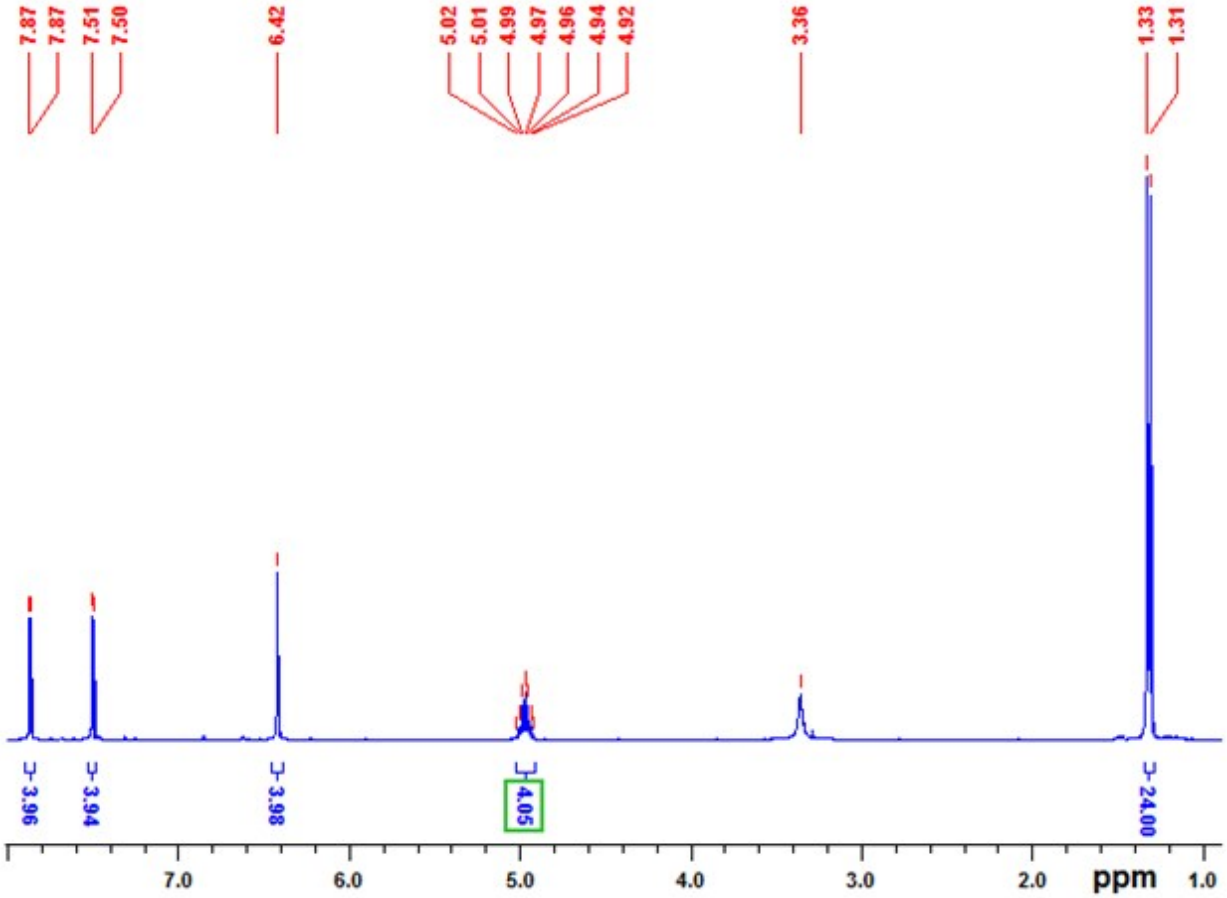

Fig. S14. ^{1}H NMR spectrum of [(mbpis)$_2$(OTf)$_2$Bi](OTf) (**4**) in DMSO-d$_6$ at RT.

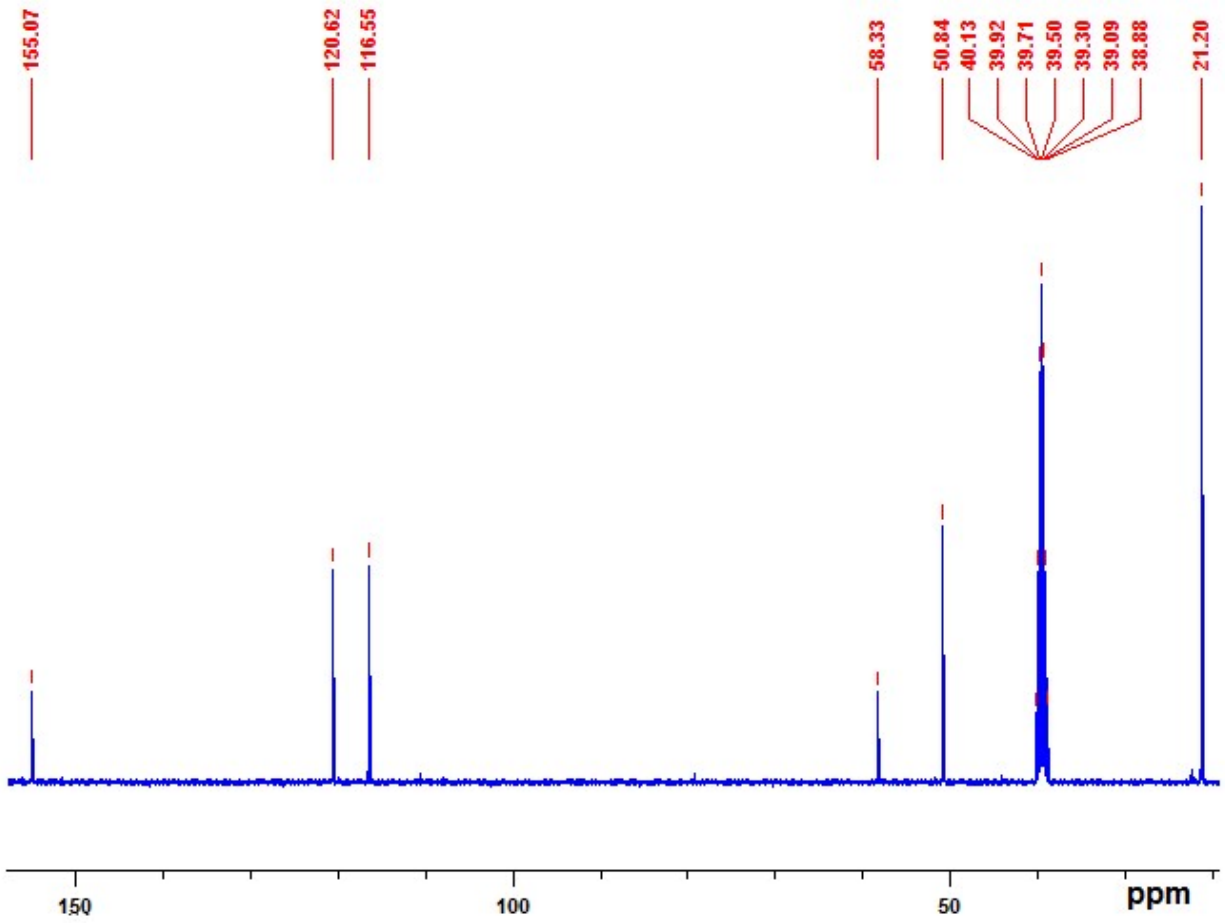

Fig. S15. ^{13}C NMR spectrum of $[(mbpis)_2(OTf)_2Bi](OTf)$ (**4**) in DMSO-d_6 at RT.

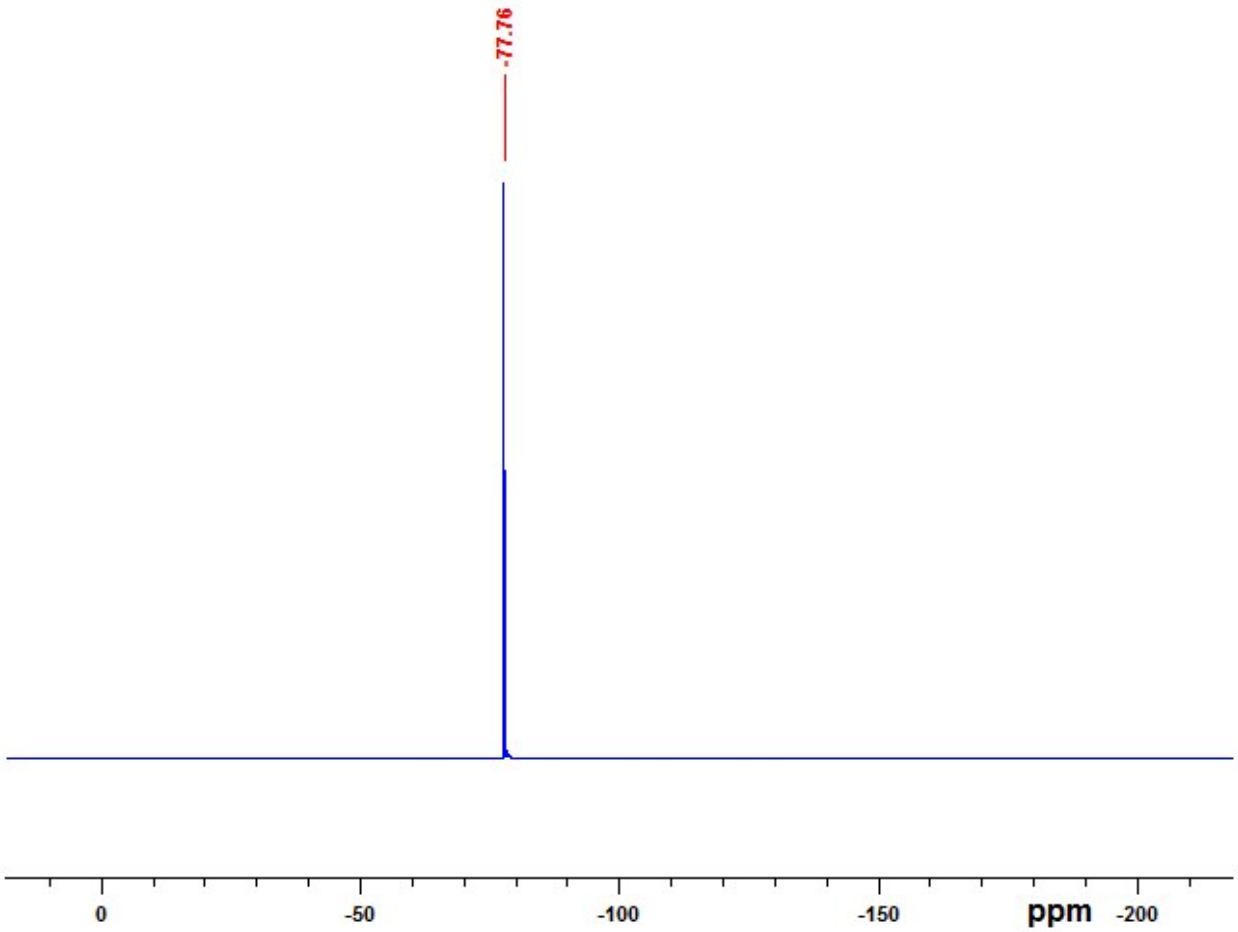

Fig. S16. ^{19}F NMR spectrum of $[(mbpis)_2(OTf)_2Bi](OTf)$ (**4**) in DMSO-d_6 at RT.

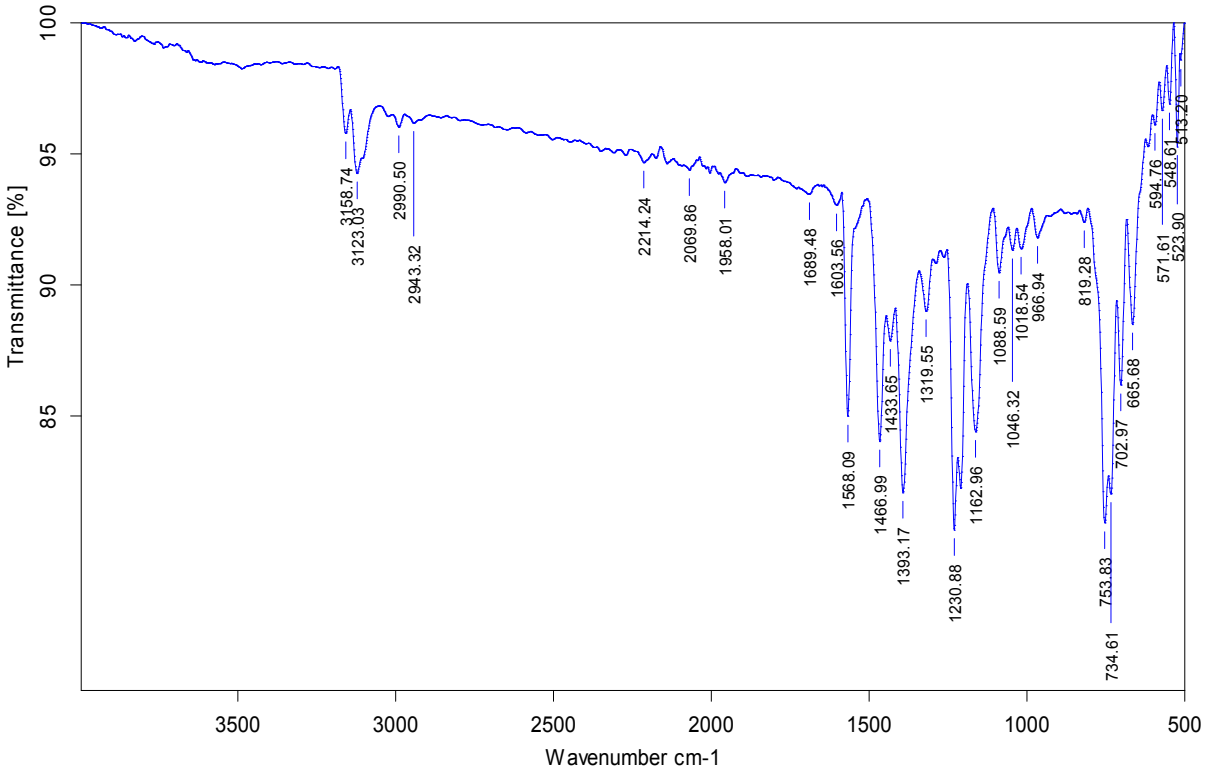

Fig. S17. Neat FT-IR spectrum of $[(mbit)_2BiCl_2][(mbit)BiCl_4]$ (**5**).

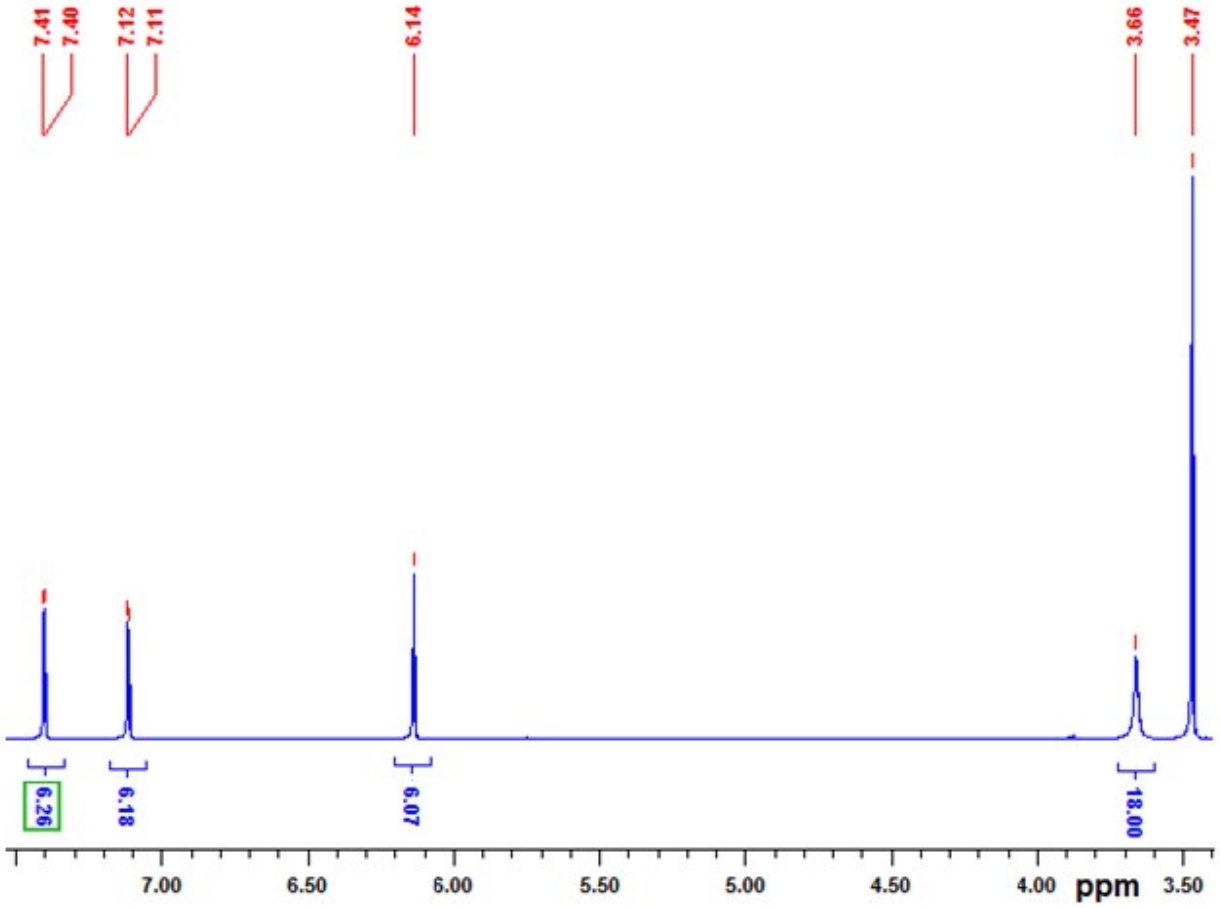

Fig. S18. ^{1}H NMR spectrum of $[(mbit)_2BiCl_2][(mbit)BiCl_4]$ (**5**) in DMSO-d_6 at RT.

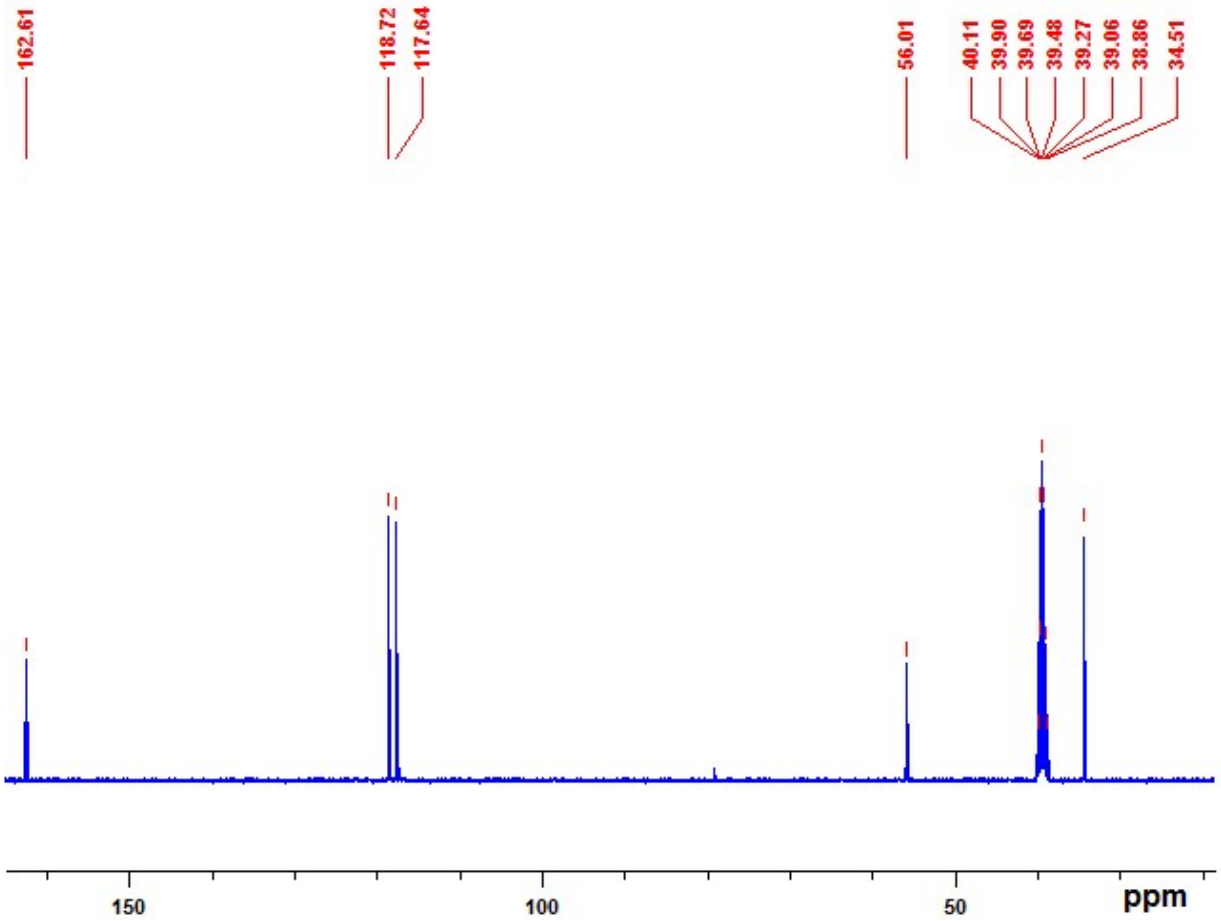

Fig. S19. ^{13}C NMR spectrum of $[(mbit)_2BiCl_2][(mbit)BiCl_4]$ (**5**) in DMSO-d_6 at RT.

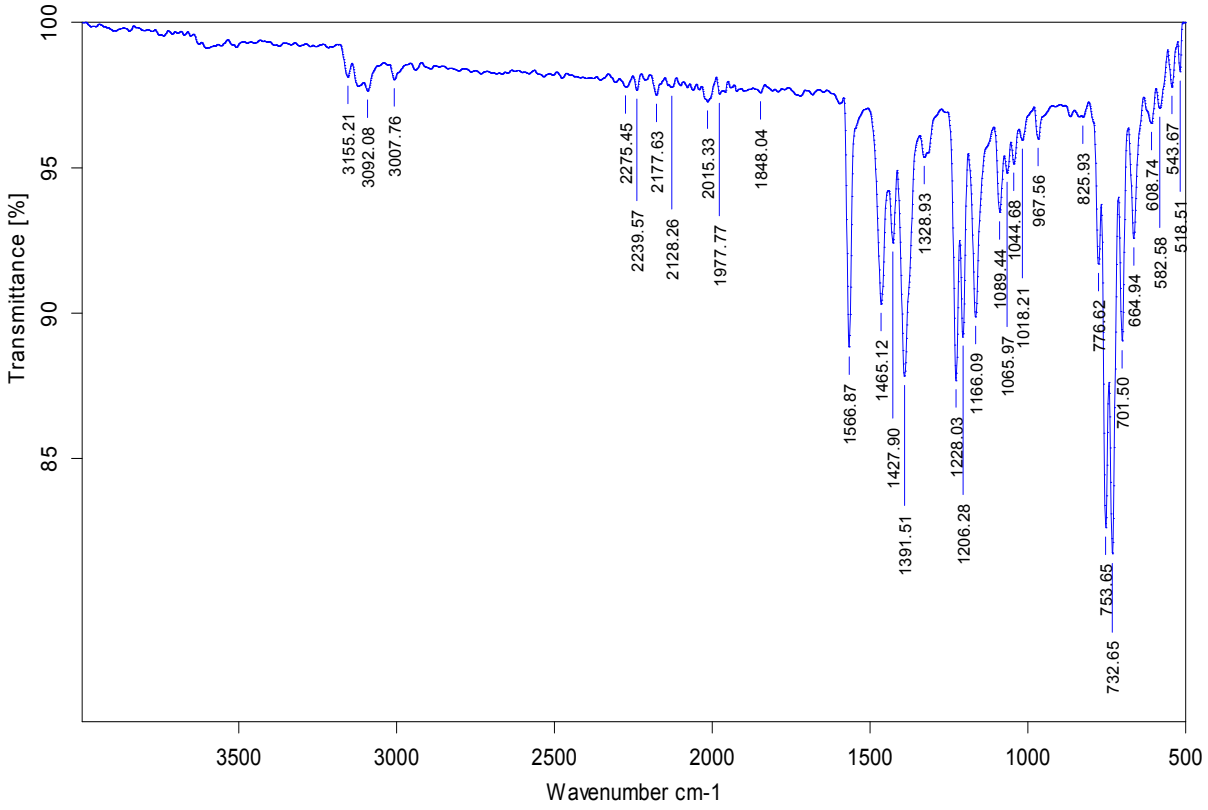

Fig. S20. Neat FT-IR spectrum of $[(mbit)Bi(Br)_2(\mu_2\text{-}Br)]_2$ (**6**).

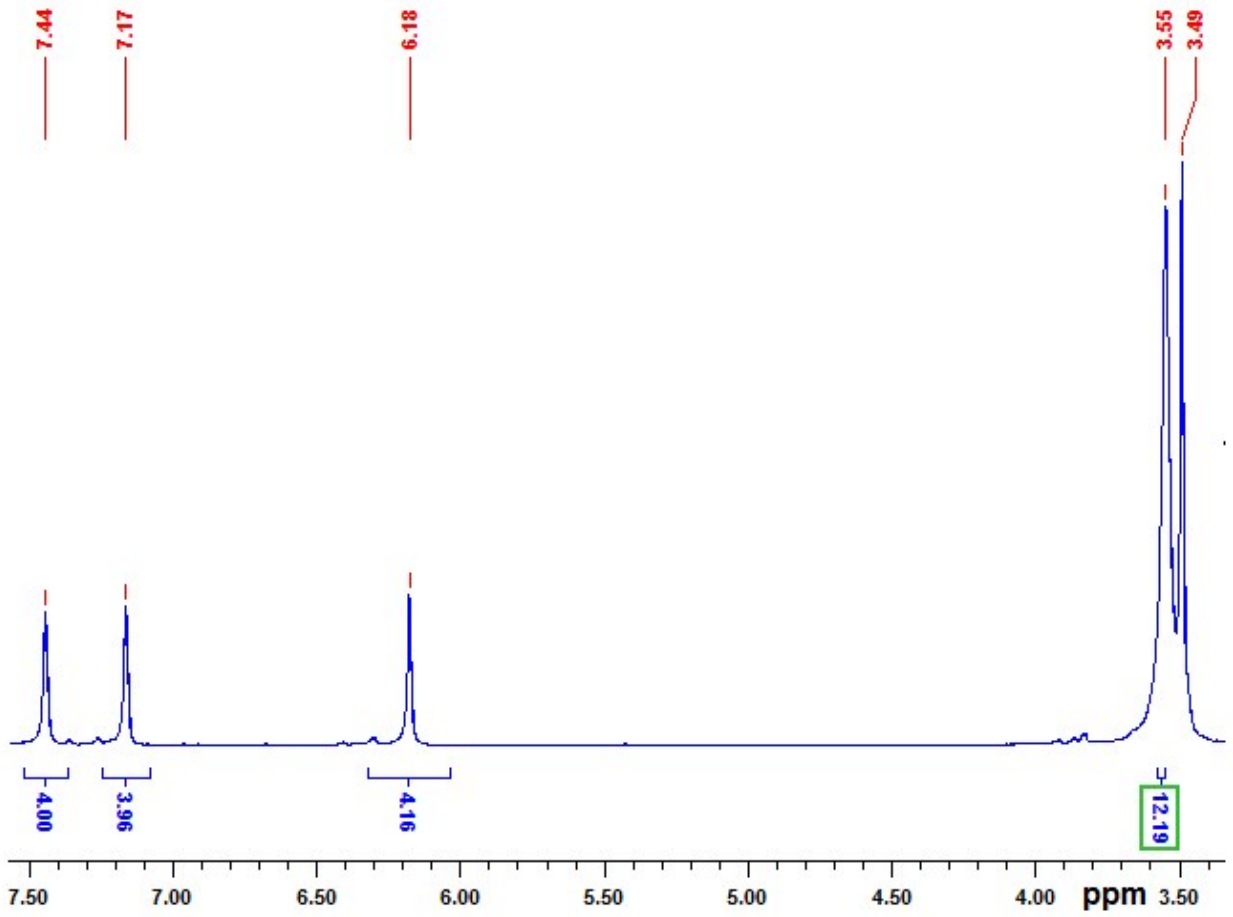

Fig. S21. ^{1}H NMR spectrum of [(mbit)Bi(Br)$_2$(μ_2-Br)]$_2$ (**6**) in DMSO-d$_6$ at RT.

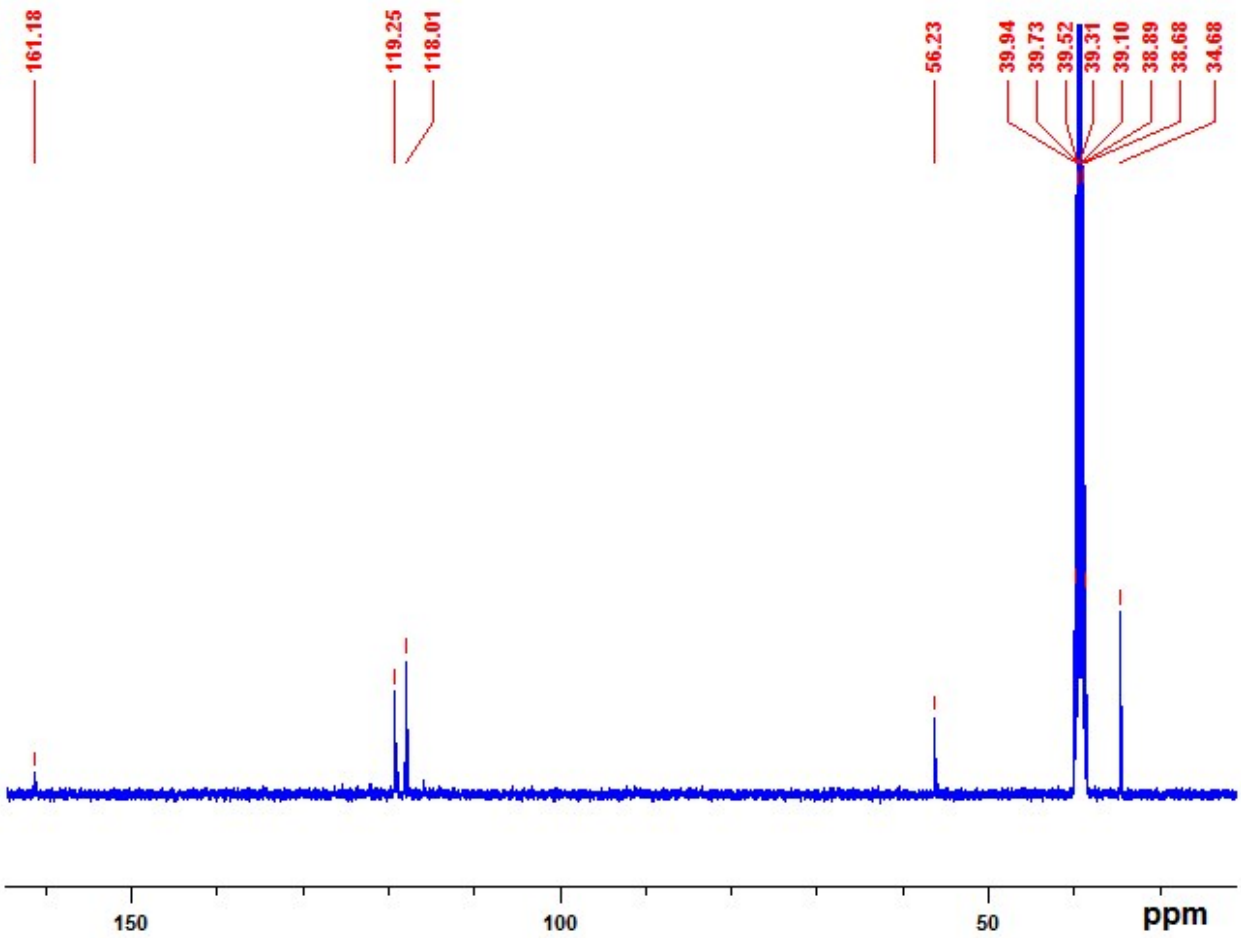

Fig. S22. ^{13}C NMR spectrum of [(mbit)Bi(Br)$_2$(μ_2-Br)]$_2$ (**6**) in DMSO-d$_6$ at RT.

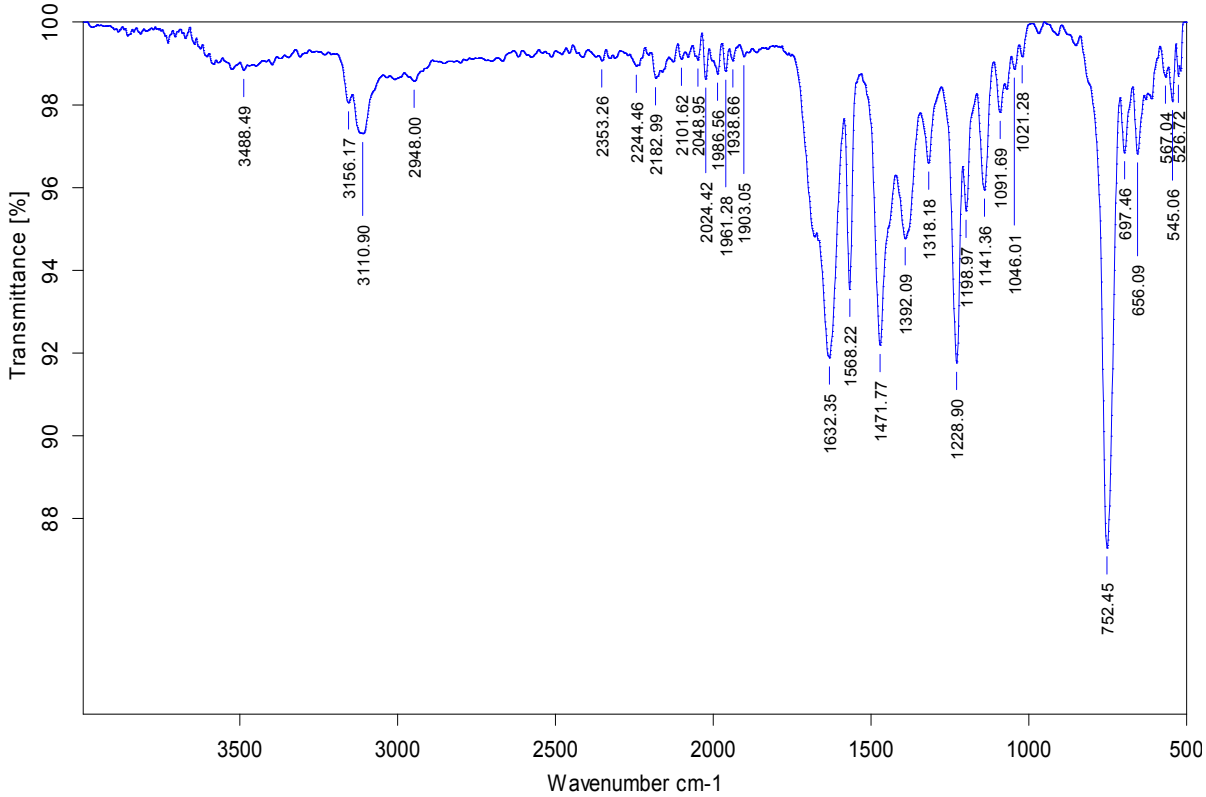

Fig. S23. Neat FT-IR spectrum of [(mbis)Bi(Cl)$_2$(μ_2-Cl)]$_2$ (**7**).

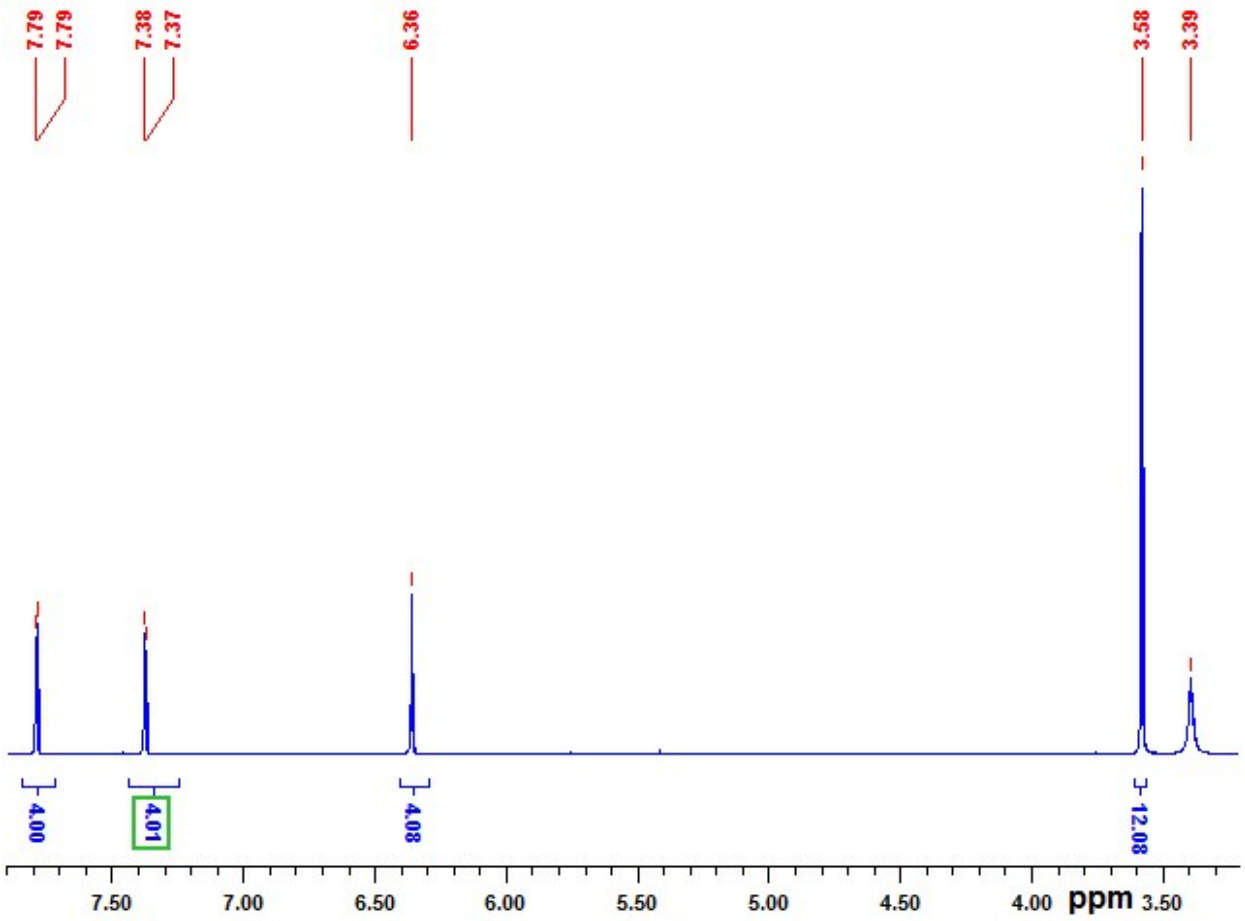

Fig. S24. ^{1}H NMR spectrum of [(mbis)Bi(Cl)$_2$(μ_2-Cl)]$_2$ (**7**) in DMSO-d$_6$ at RT.

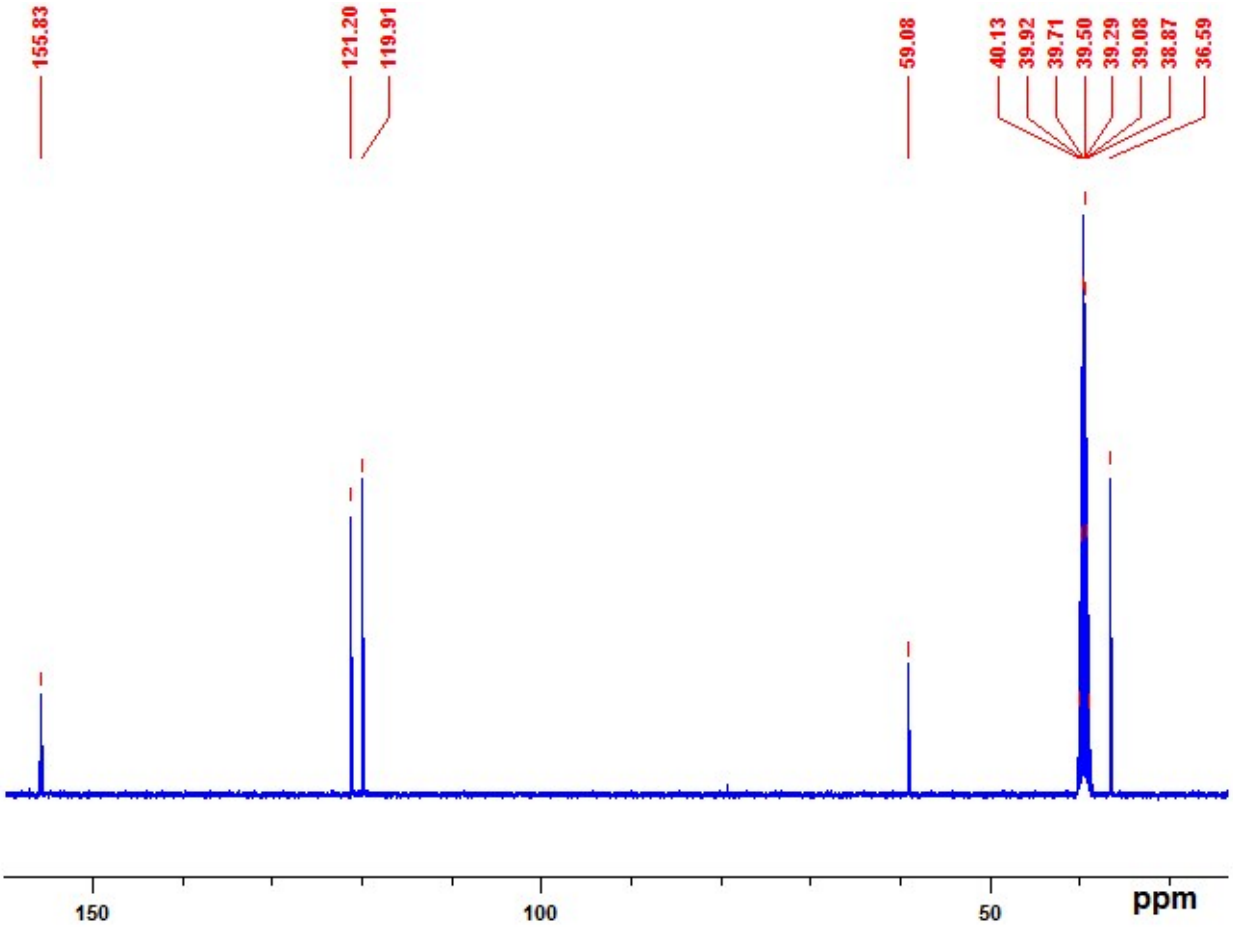

Fig. S25. ^{13}C NMR spectrum of [(mbis)Bi(Cl)$_2$(μ_2-Cl)]$_2$ (**7**) in DMSO-d$_6$ at RT.

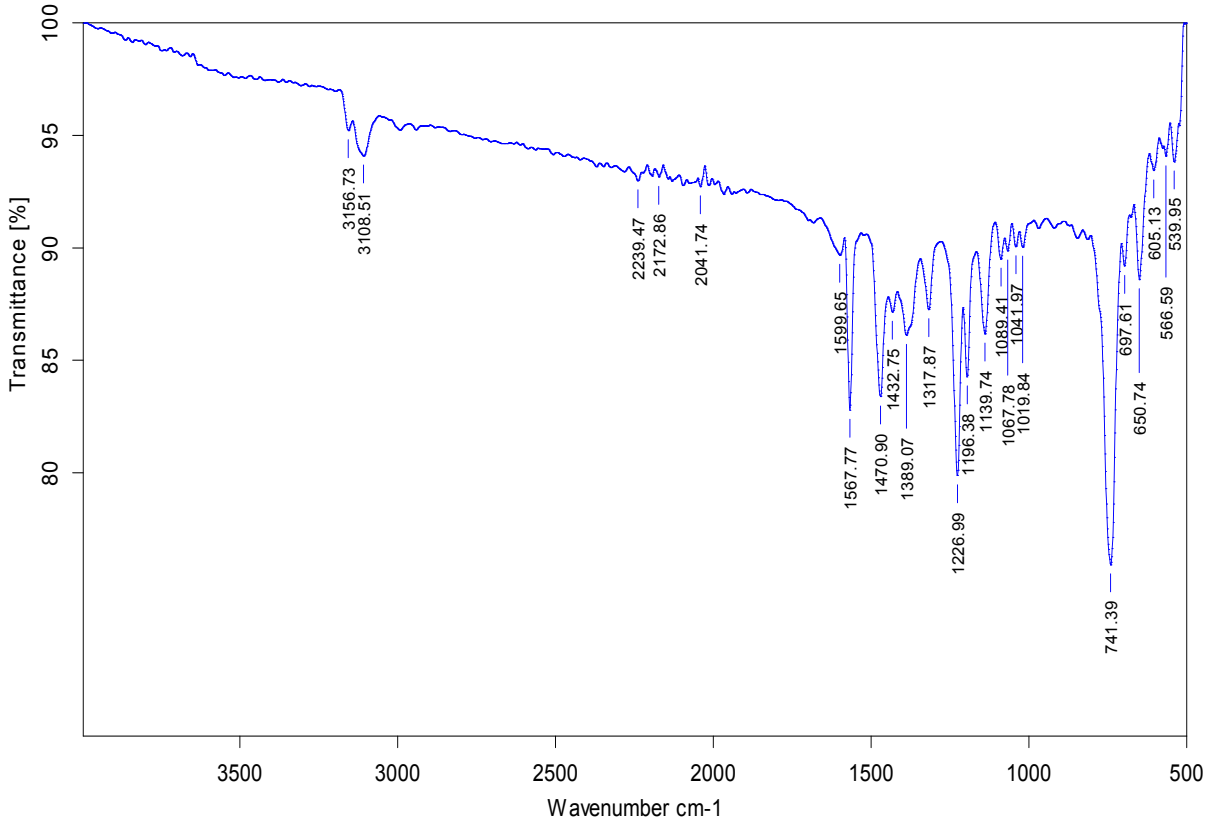

Fig. S26. Neat FT-IR spectrum of [(mbis)Bi(Br)$_2$(μ_2-Br)]$_2$ (**8**).

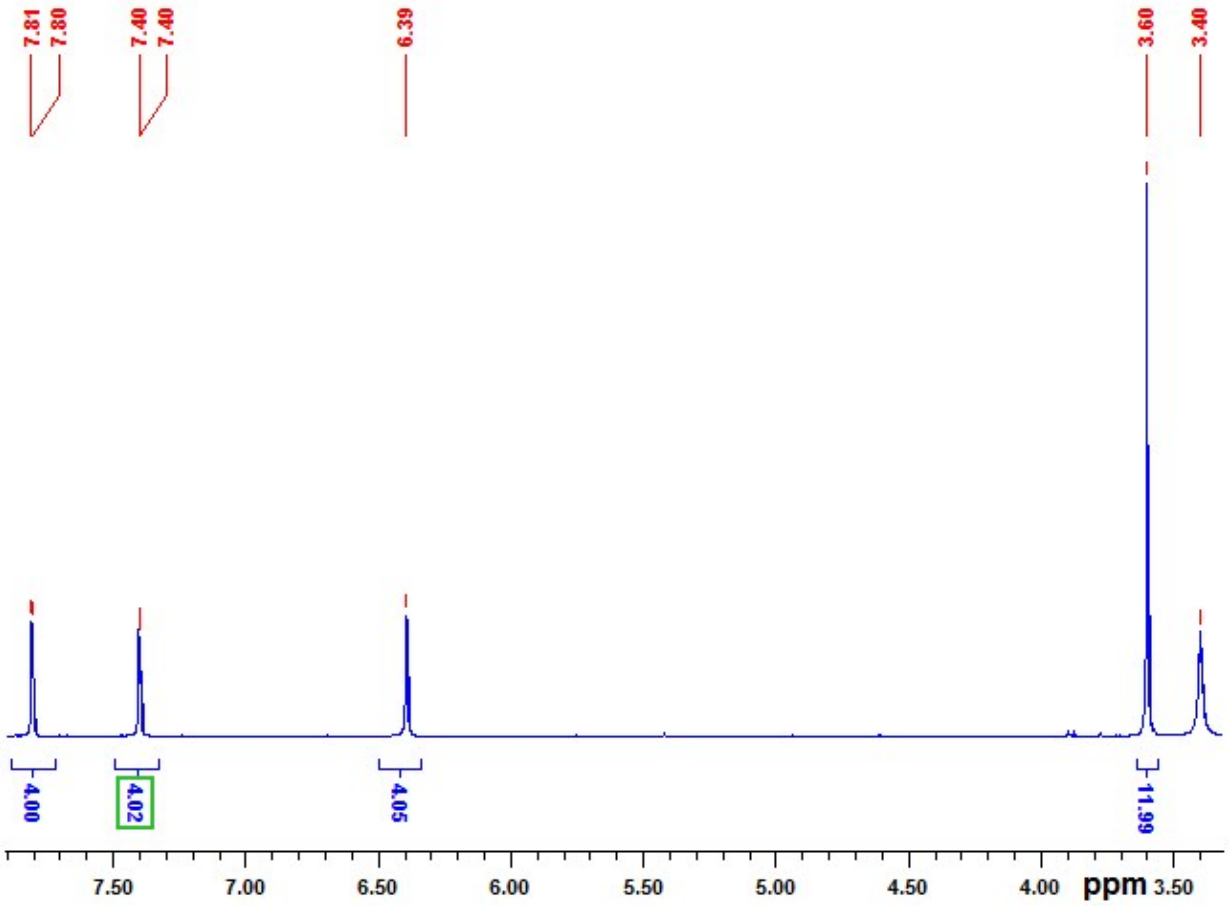

Fig. S27. ^{1}H NMR spectrum of [(mbis)Bi(Br)$_2$(μ_2-Br)]$_2$ (**8**) in DMSO-d$_6$ at RT.

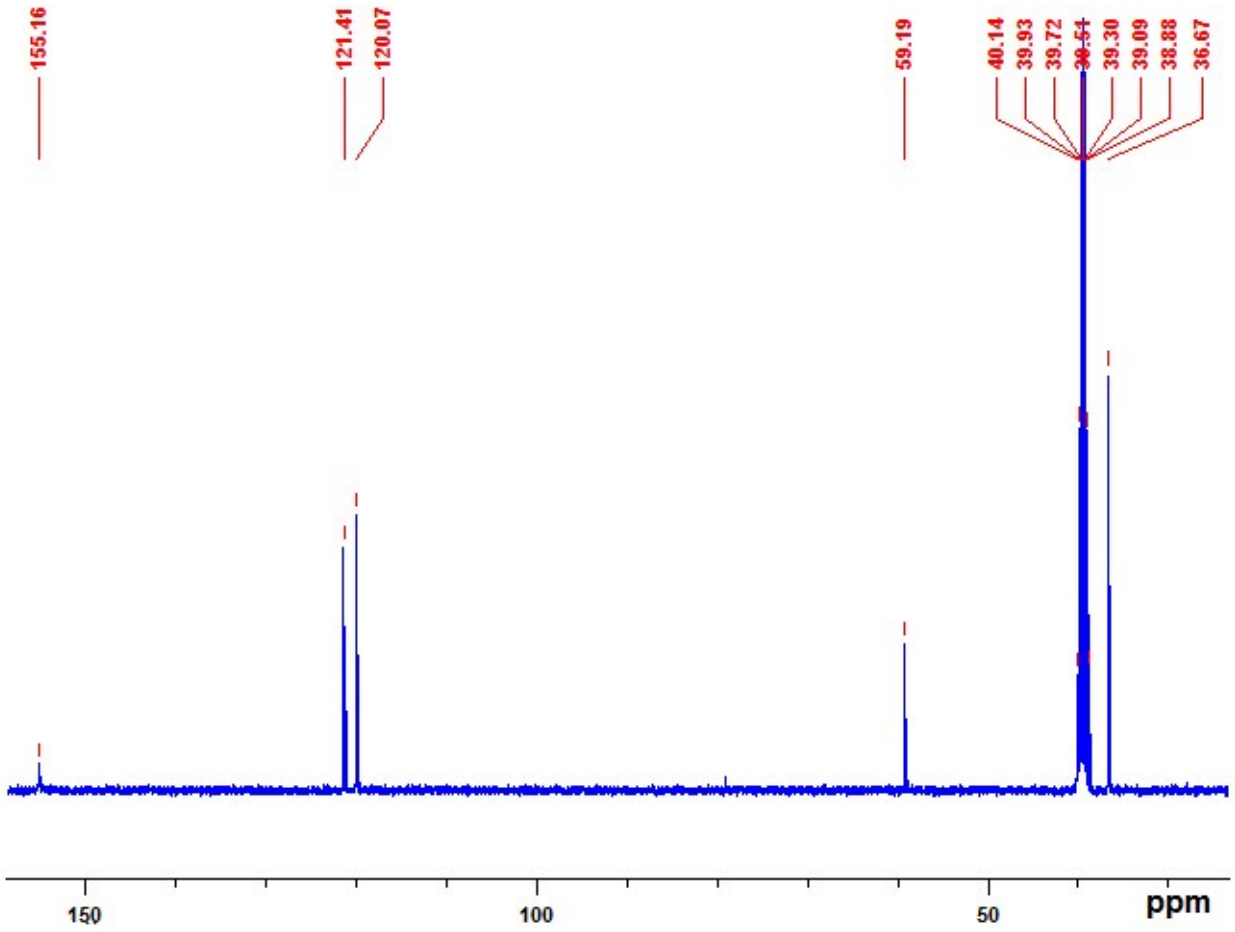

Fig. S28. ^{13}C NMR spectrum of [(mbis)Bi(Br)$_2$(μ_2-Br)]$_2$ (**8**) in DMSO-d$_6$ at RT.

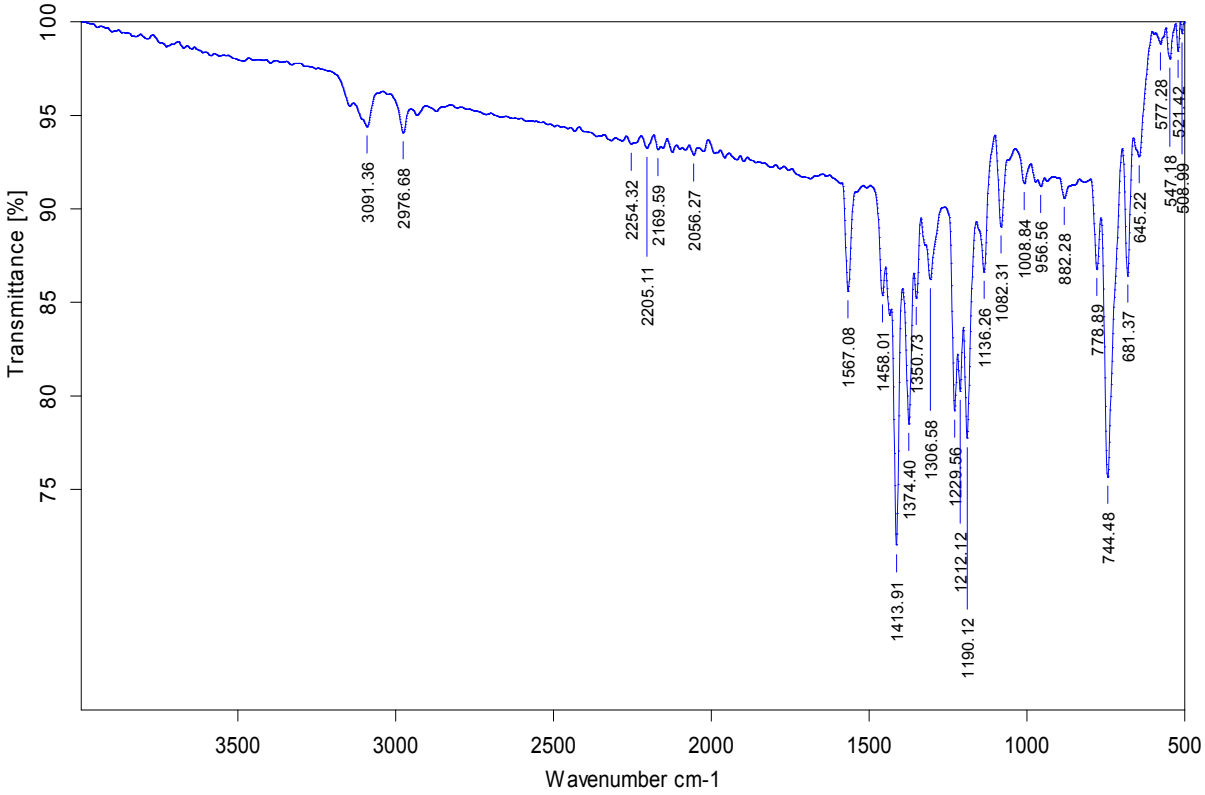

Fig. S29. Neat FT-IR spectrum of [(mbpit)Bi(Cl)$_2$(μ_2-Cl)]$_2$.CH$_3$CN (**9**).

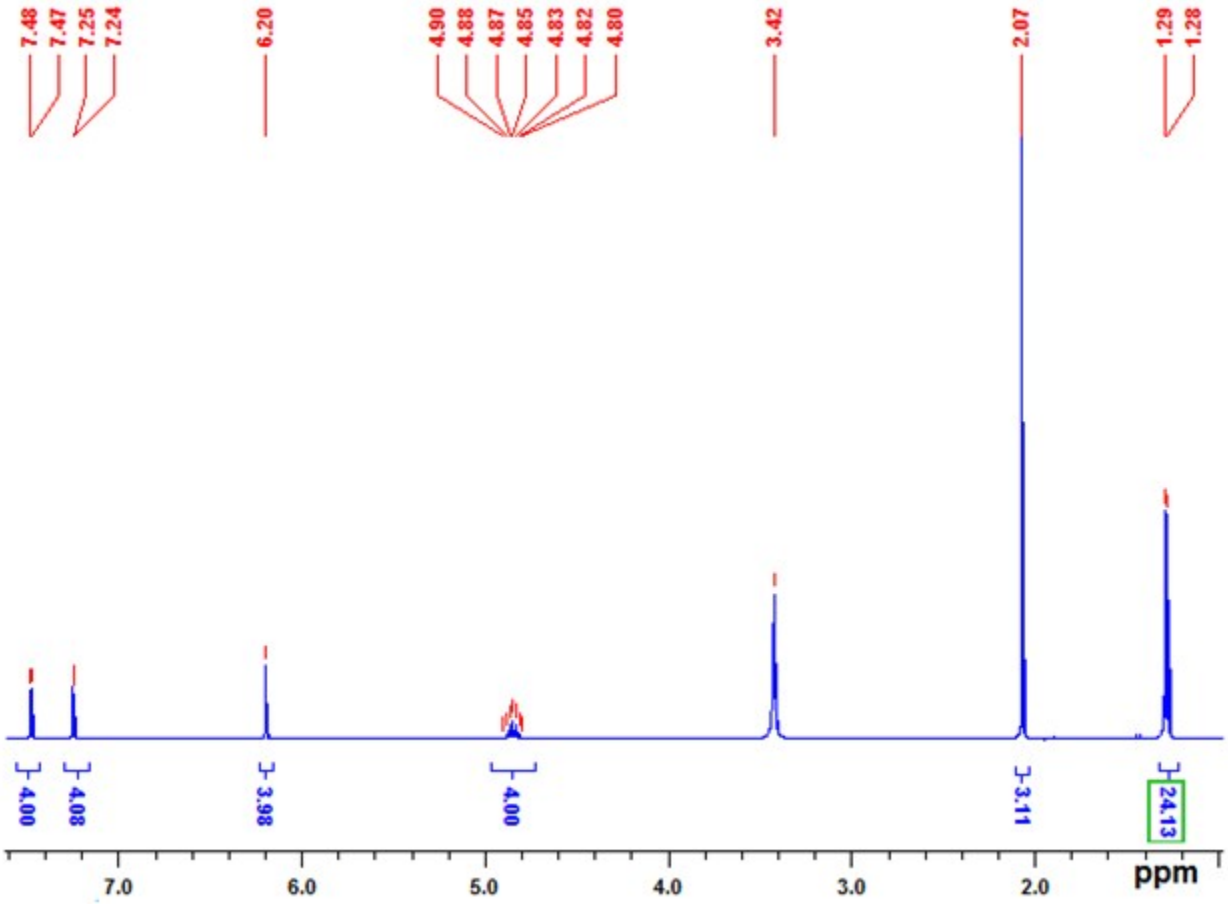

Fig. S30. ^{1}H NMR spectrum of [(mbpit)Bi(Cl)$_2$(μ_2-Cl)]$_2$.CH$_3$CN (**9**) in DMSO-d$_6$ at RT.

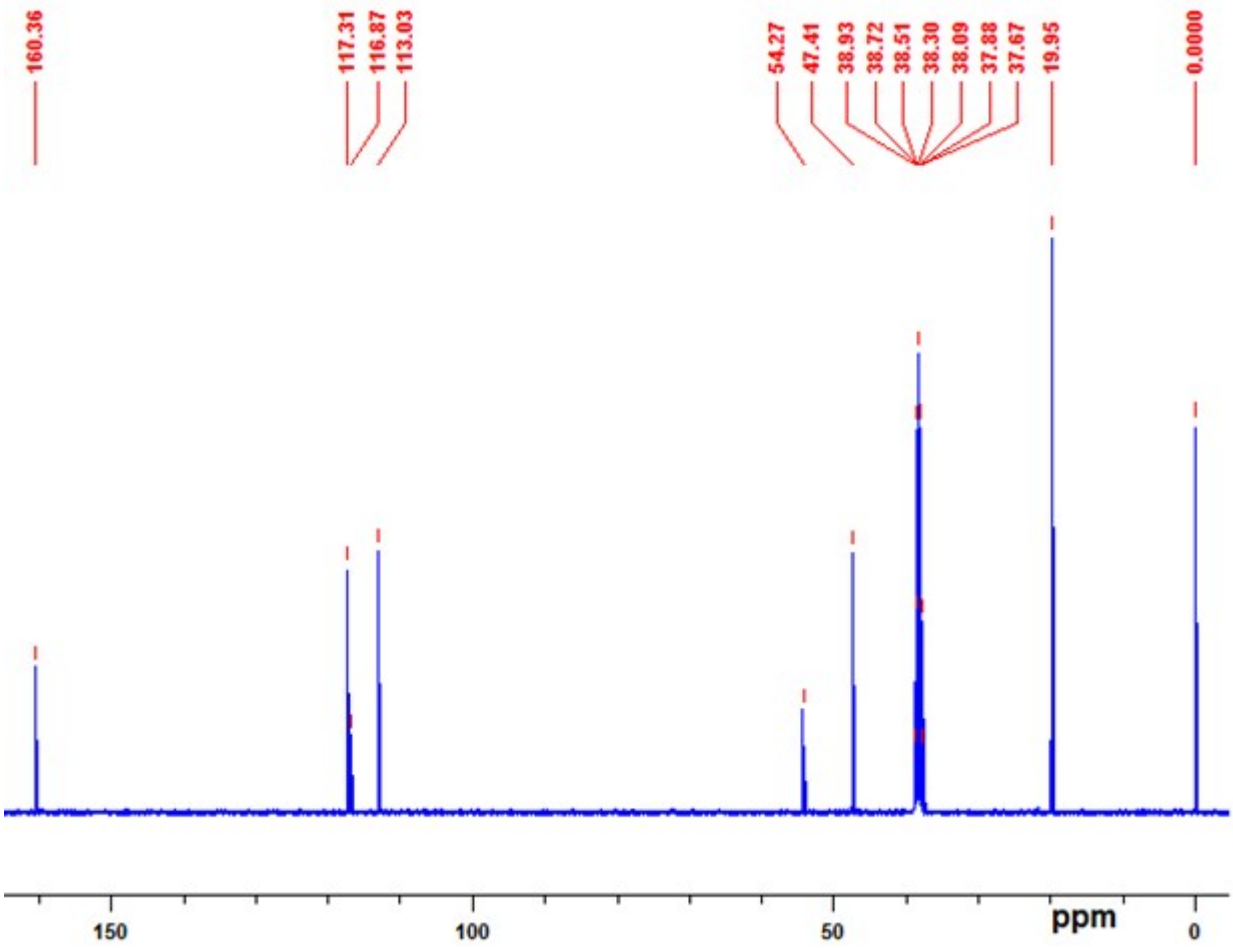

Fig. S31. ^{13}C NMR spectrum of [(mbpit)Bi(Cl)$_2$(μ_2-Cl)]$_2$.CH$_3$CN (**9**) in DMSO-d$_6$ at RT.

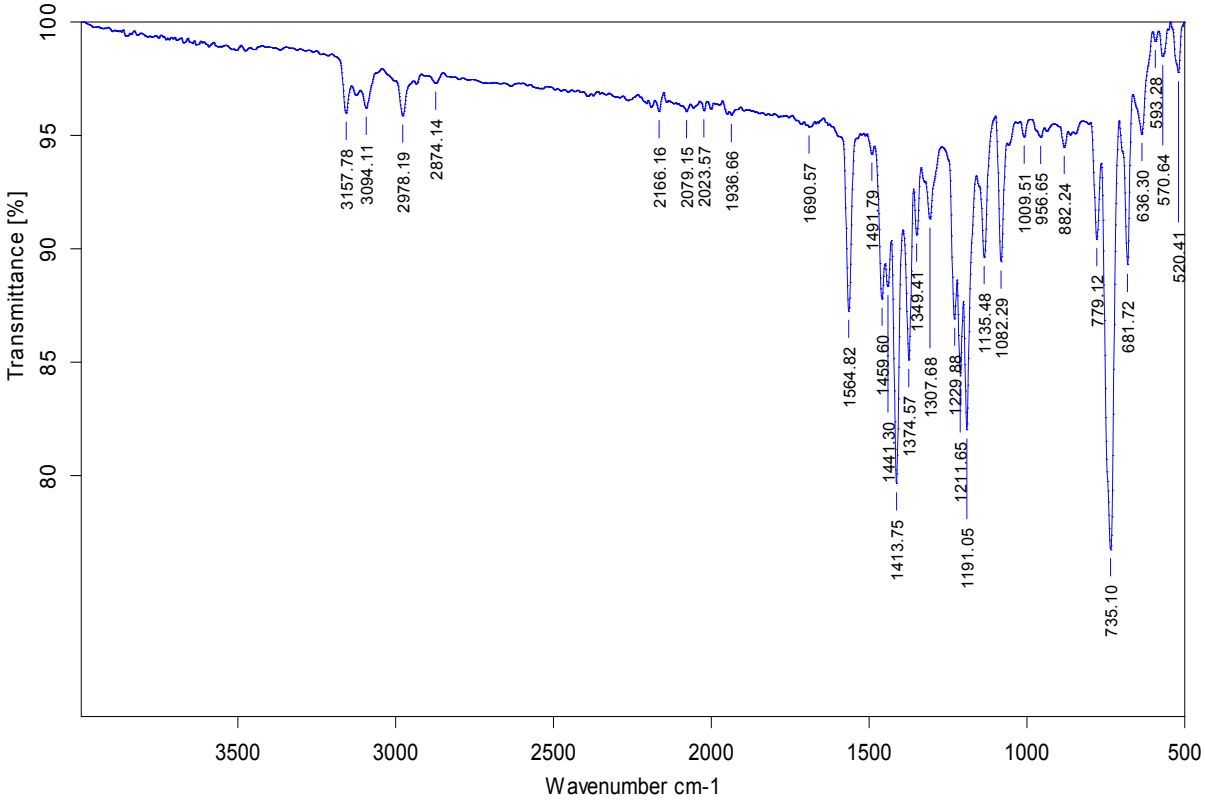

Fig. S32. Neat FT-IR spectrum of [(mbpit)Bi(Br)$_2$(μ_2-Br)]$_2$.CH$_3$CN (**10**).

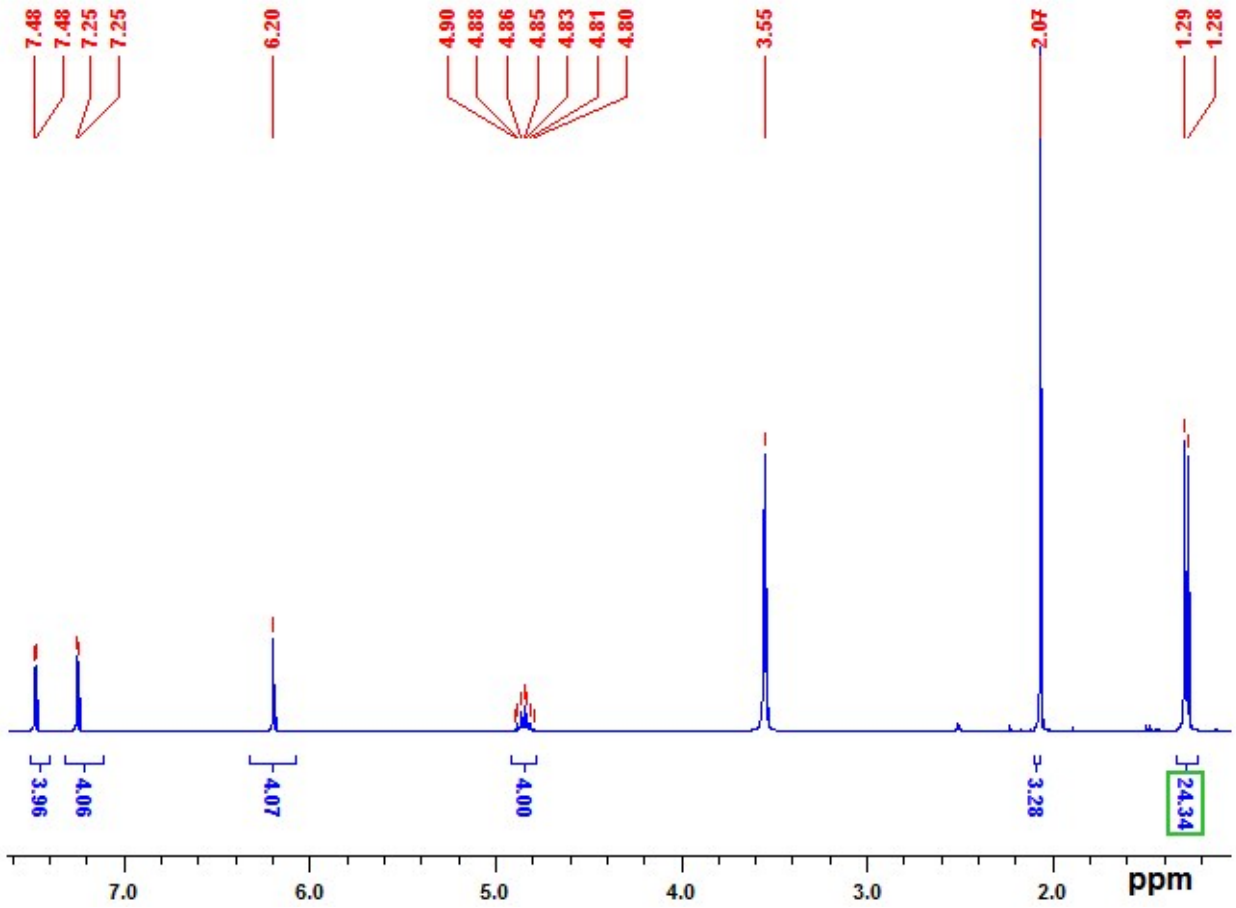

Fig. S33. ^{1}H NMR spectrum of [(mbpit)Bi(Br)$_2$(μ_2-Br)]$_2$.CH$_3$CN (**10**) in DMSO-d$_6$ at RT.

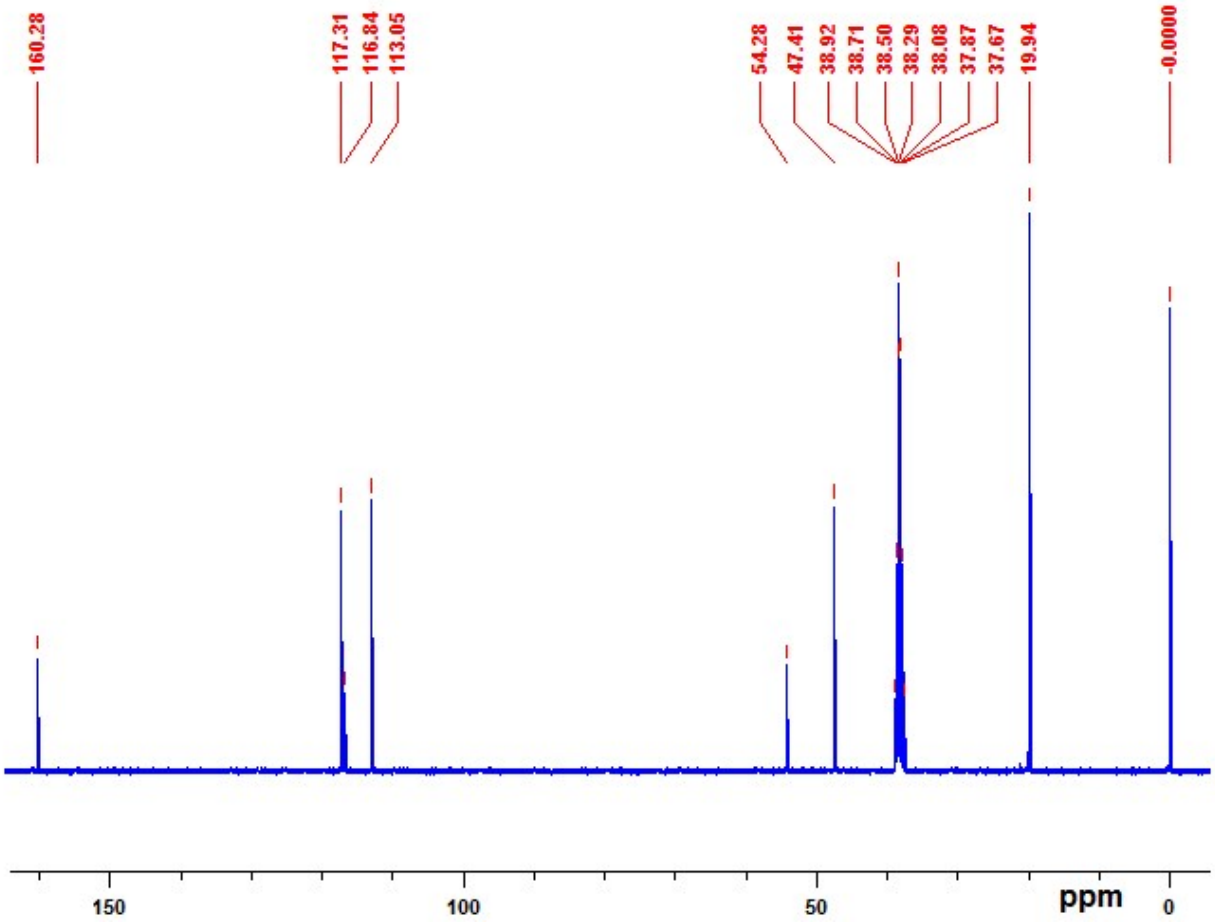

Fig. S34. ^{13}C NMR spectrum of [(mbpit)Bi(Br)$_2$(μ_2-Br)]$_2$.CH$_3$CN (**10**) in DMSO-d$_6$ at RT.

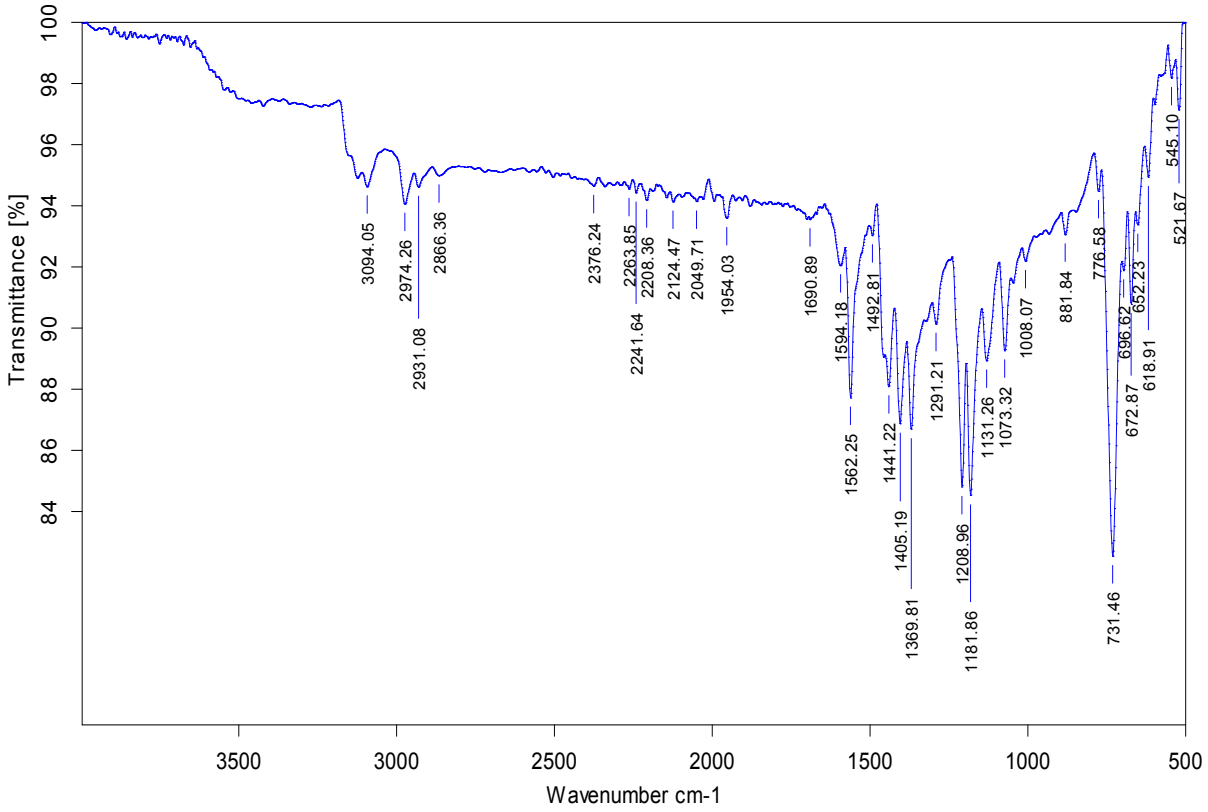

Fig. S35. Neat FT-IR spectrum of [(mbpis)Bi(Cl)$_2$(μ_2-Cl)]$_2$.CH$_3$CN (**11**).

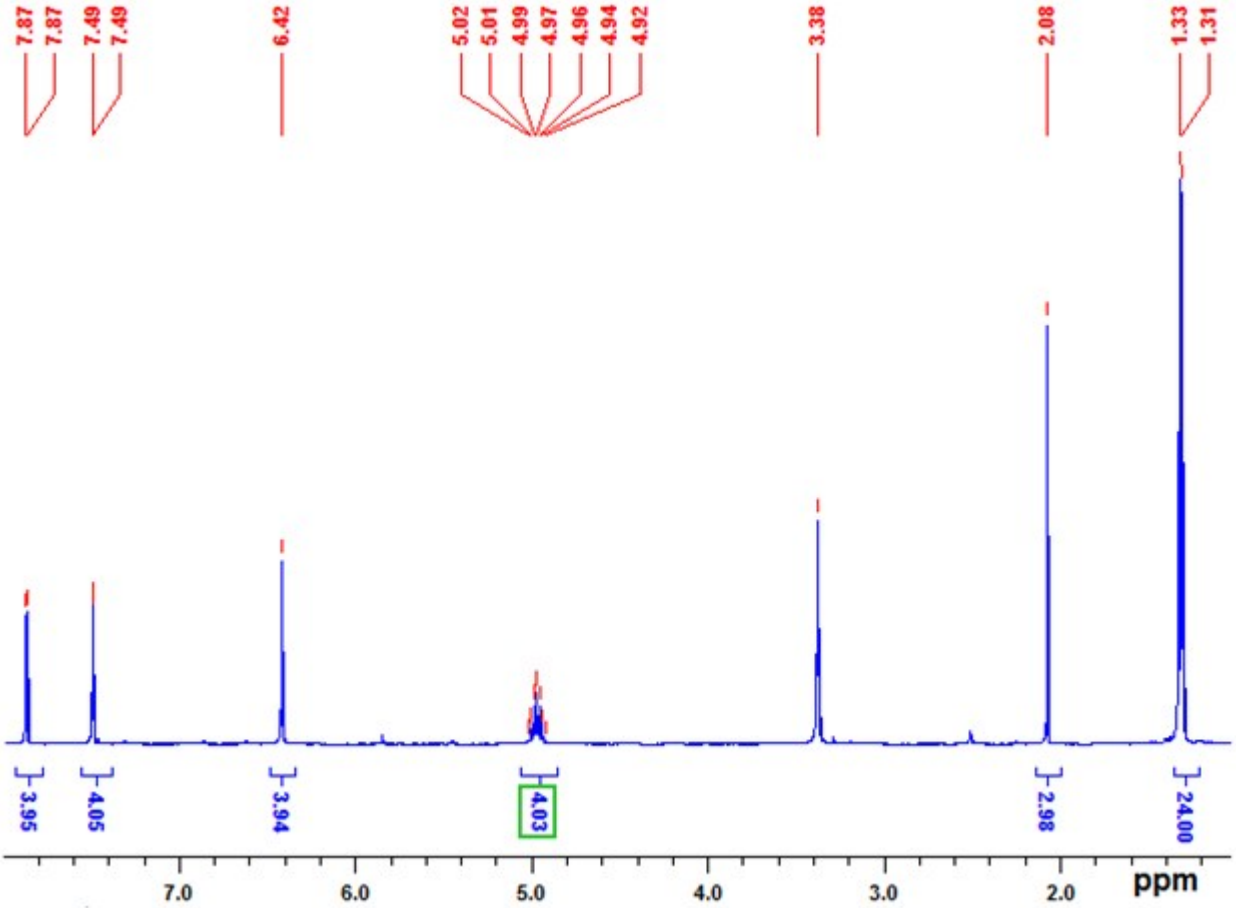

Fig. S36. ^{1}H NMR spectrum of [(mbpis)Bi(Cl)$_2$(μ_2-Cl)]$_2$.CH$_3$CN (**11**) in DMSO-d$_6$ at RT.

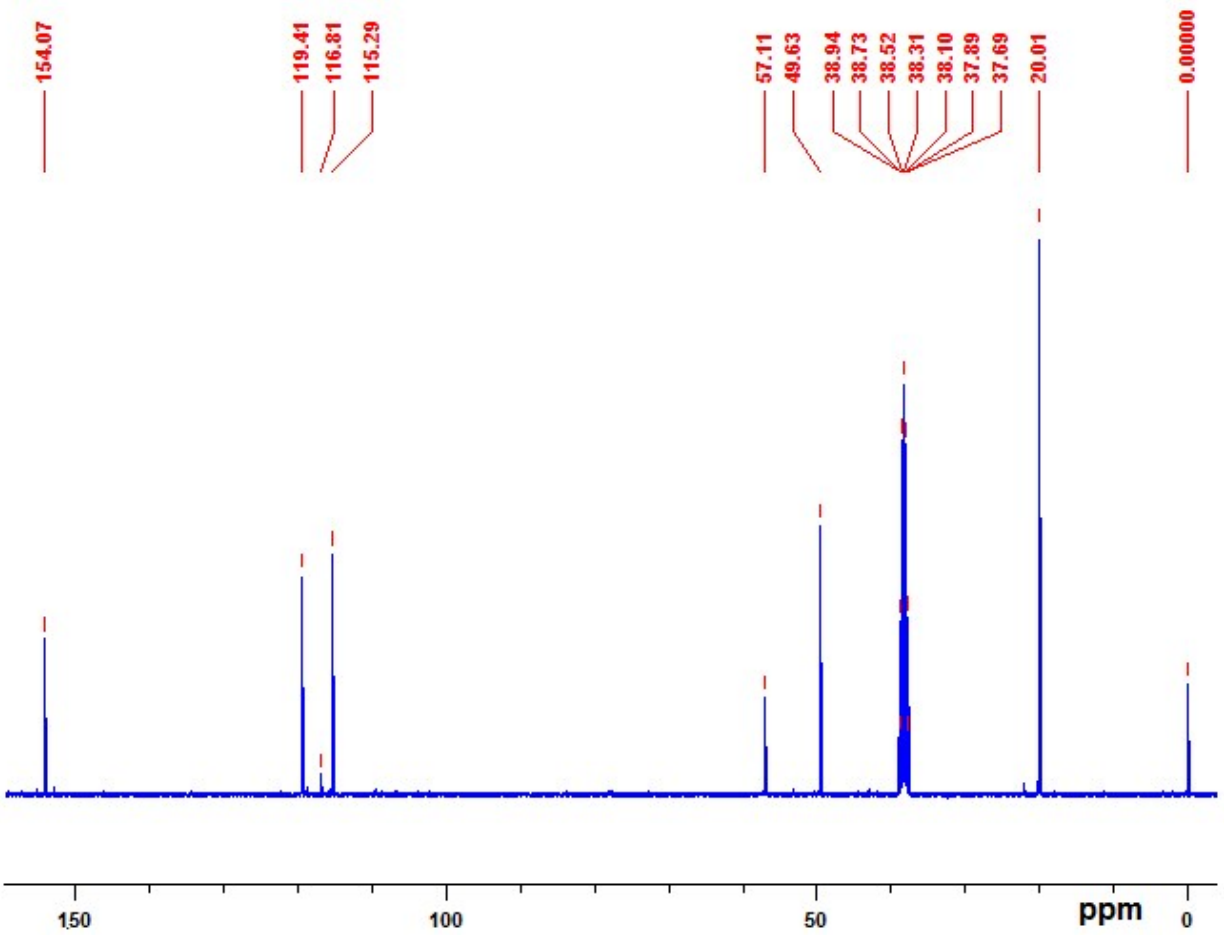

Fig. S37. ^{13}C NMR spectrum of [(mbpis)Bi(Cl)$_2$(μ_2-Cl)]$_2$.CH$_3$CN (**11**) in DMSO-d$_6$ at RT.

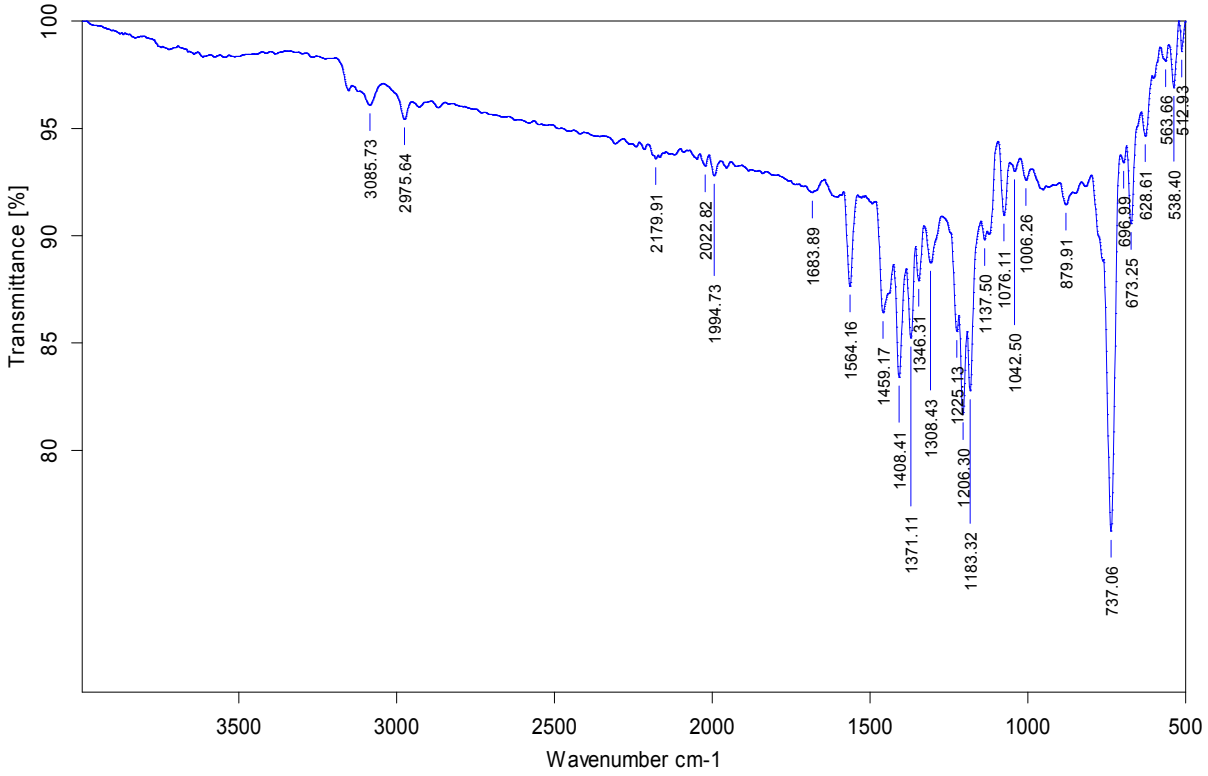

Fig. S38. Neat FT-IR spectrum of $[(mbpis)Bi(Br)_2(\mu_2\text{-}Br)]_2.CH_3CN$ (**12**).

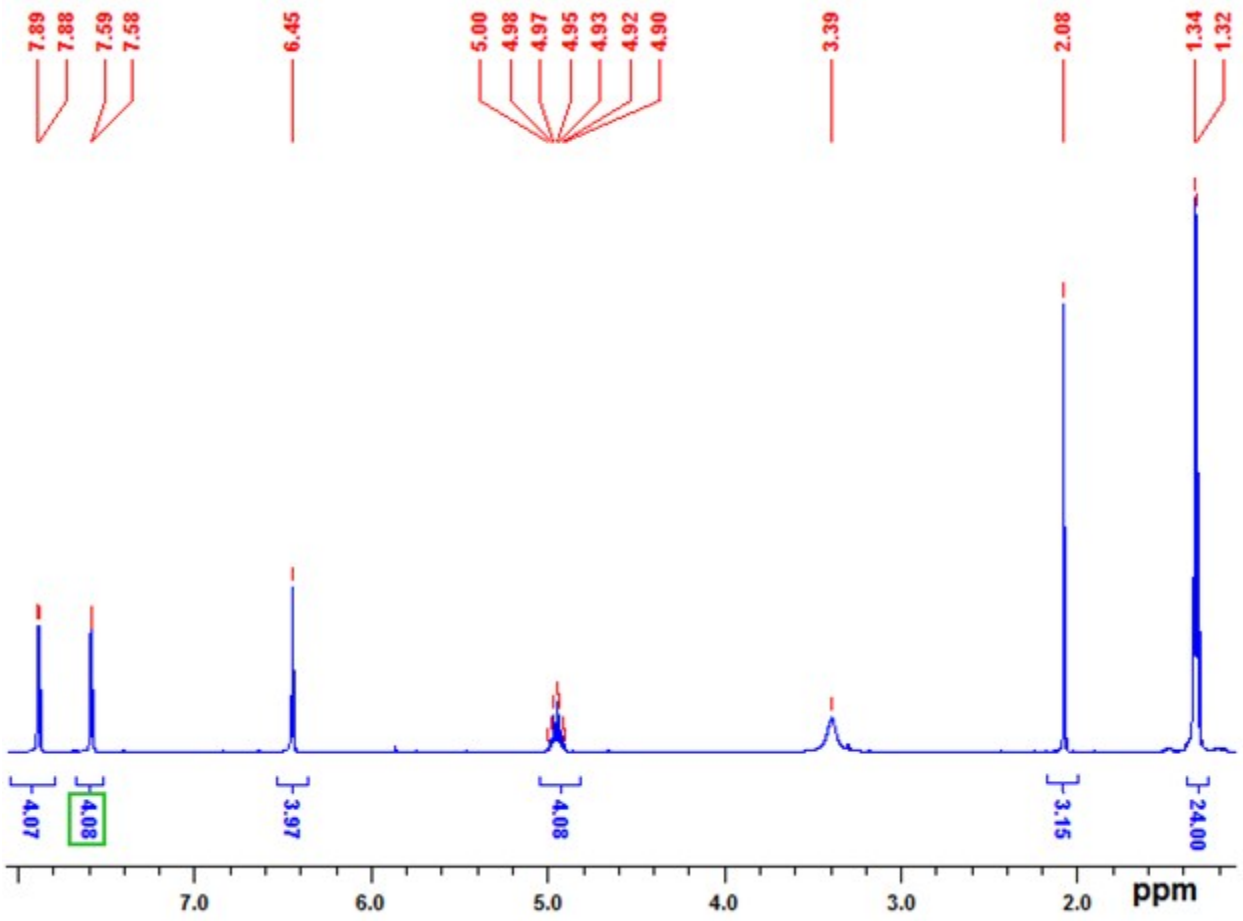

Fig. S39. ^{1}H NMR spectrum of [(mbpis)Bi(Br)$_2$(μ_2-Br)]$_2$.CH$_3$CN (**12**) in DMSO-d$_6$ at RT.

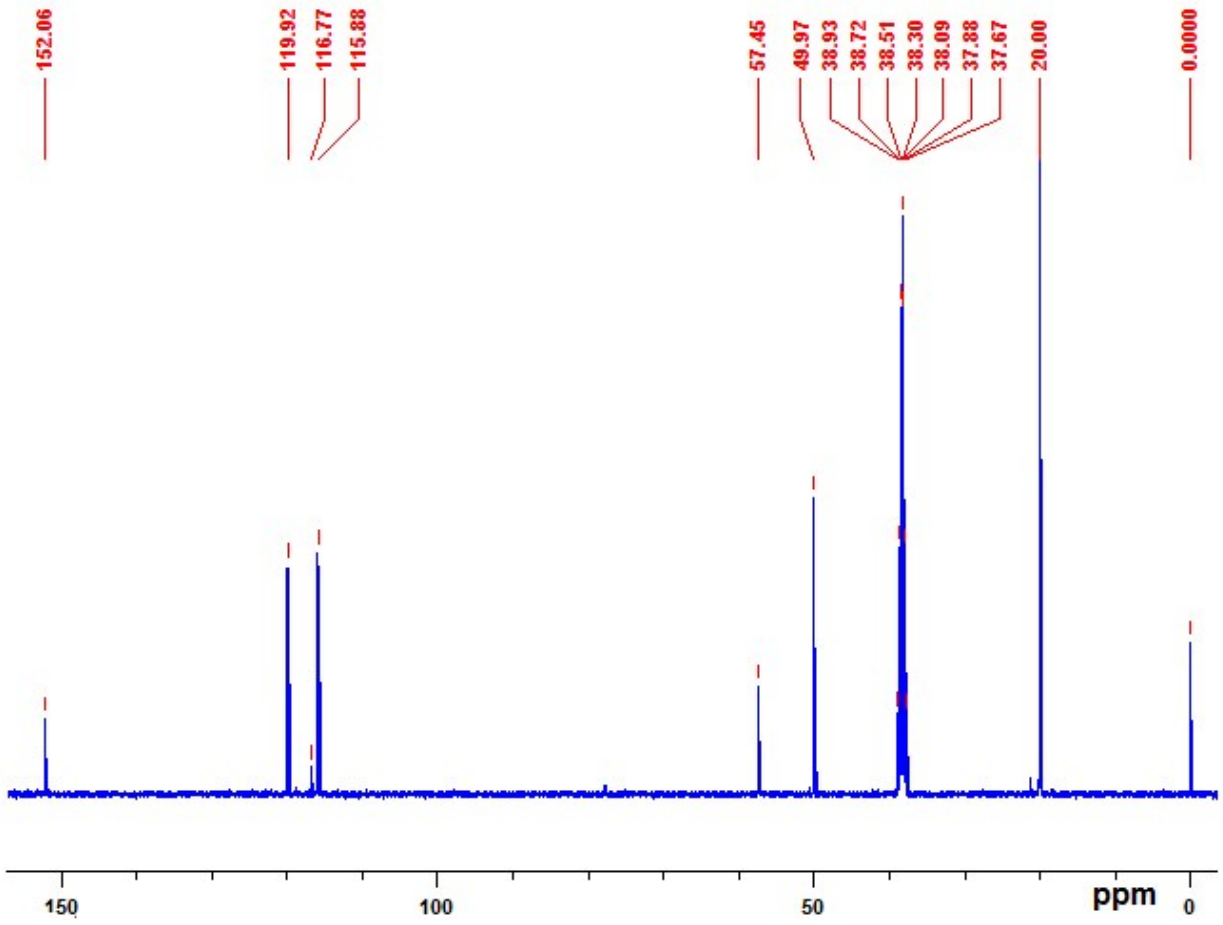

Fig. S40. ^{13}C NMR spectrum of $[(mbpis)Bi(Br)_2(\mu_2\text{-}Br)]_2.CH_3CN$ (**12**) in DMSO-d_6 at RT.

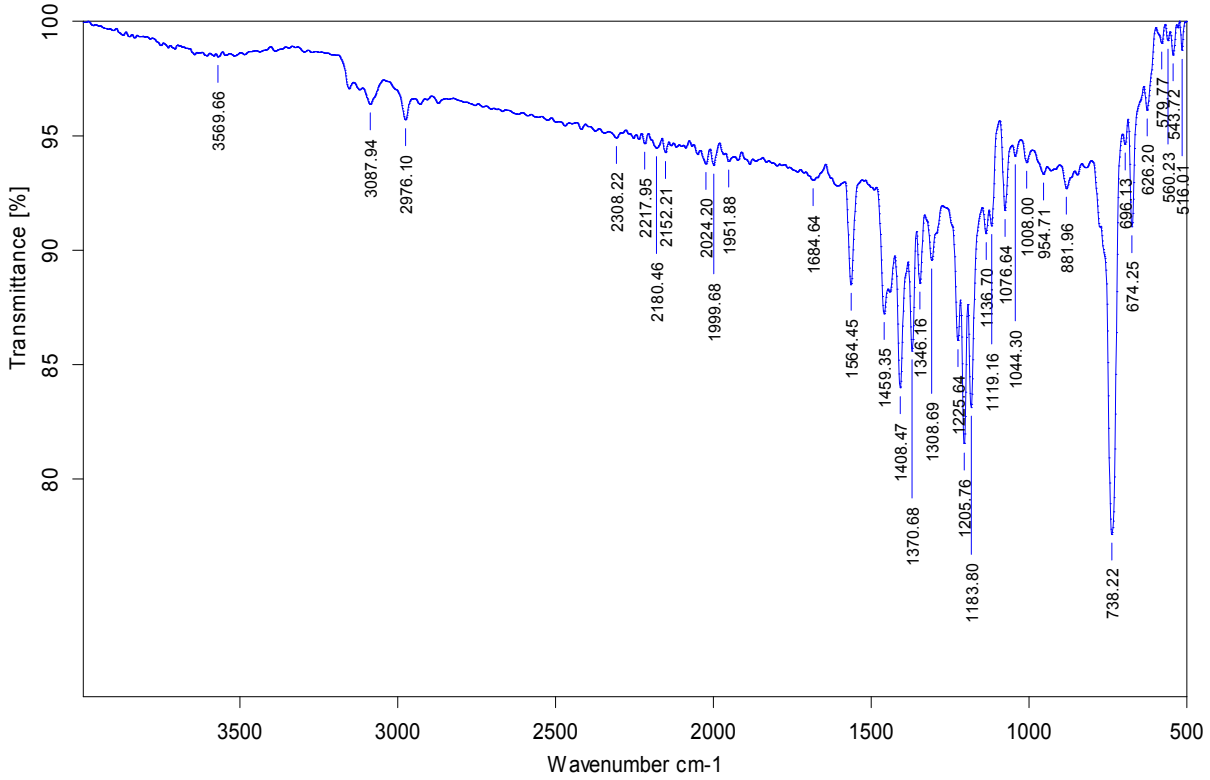

Fig. S41. Neat FT-IR spectrum of $[(mbpis)Bi_2(Br)_3(\mu_2\text{-}Br_2)(\mu_3\text{-}Br)]_2.CH_3CN$ (**13**).

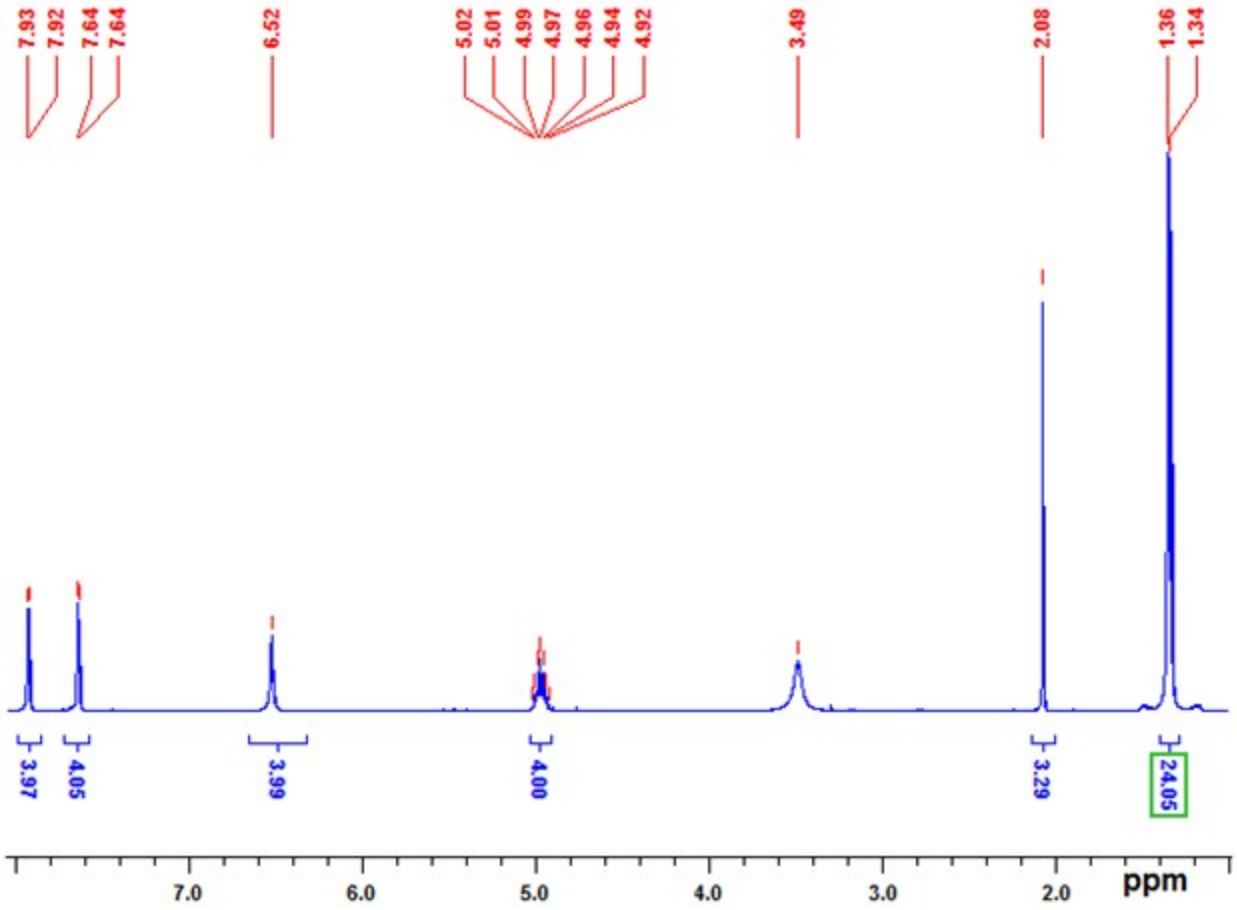

Fig. S42. ^{1}H NMR spectrum of [(mbpis)$Bi_2(Br)_3(\mu_2\text{-}Br_2)(\mu_3\text{-}Br)]_2.CH_3CN$ (**13**) in DMSO-d_6 at RT.

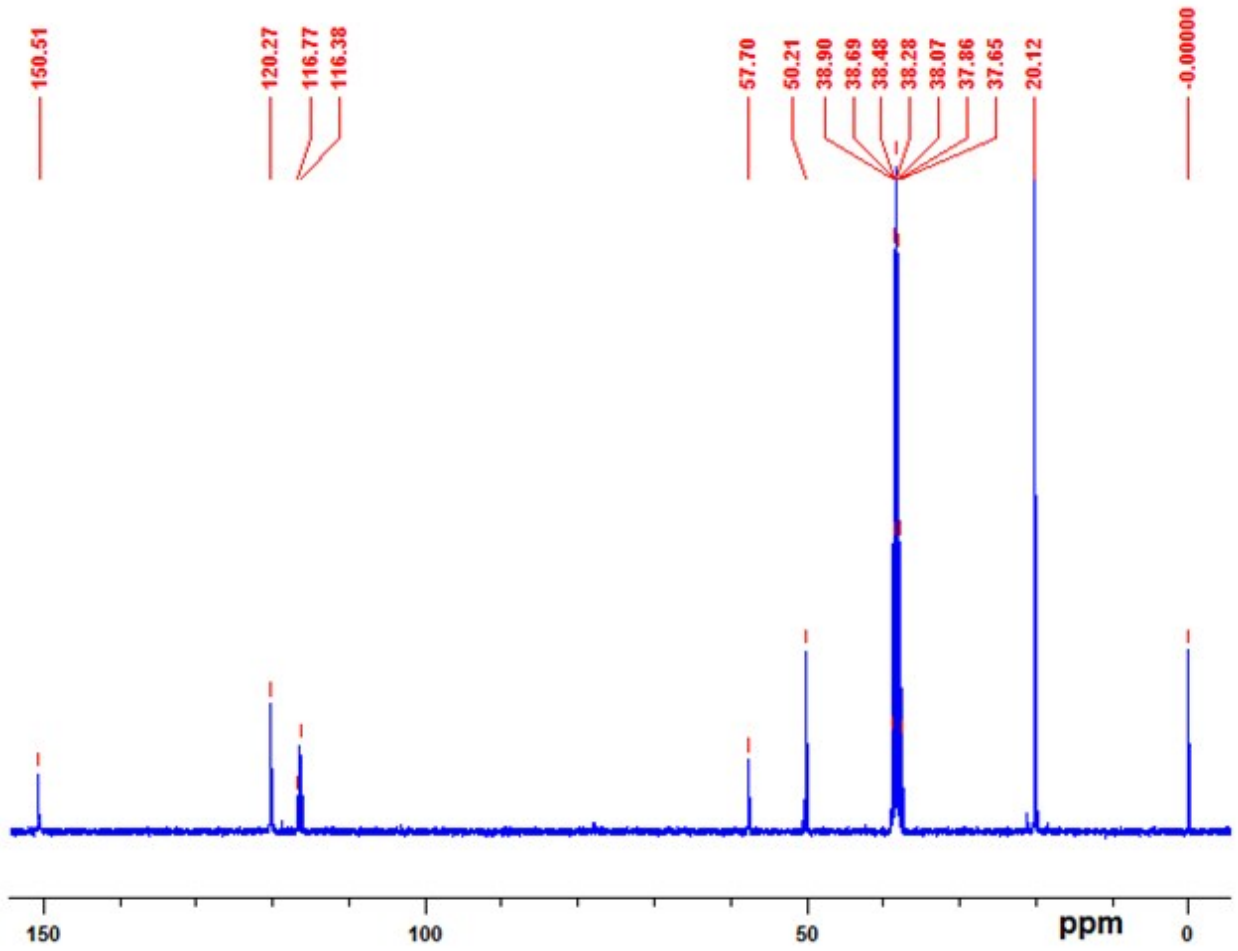

Fig. S43. ^{13}C NMR spectrum of [(mbpis)$Bi_2(Br)_3(\mu_2\text{-}Br_2)(\mu_3\text{-}Br)]_2.CH_3CN$ (**13**) in DMSO-d_6 at RT.

Catalysts 1-13 promoted triaryl- or tryheteroaryl methanes synthesis

The newly isolated bismuth(III) catalysts (**1**-**13**) were utilized for the synthesis of triaryl and tryheteroaryl methanes under very mild conditions. Bismuth(III) complex (0.050 mmol) was taken in a test tube along with arene or heteroarene (0.100 mmol) in toluene (0.50 mL) under ambient condition. Subsequently, the mixture was stirred at room temperature for 2-3 min followed by the addition of aromatic aldehyde (0.050 mmol). Finally, test tube wall was washed with toluene (0.50 mL) and allowed to stir at room temperature. The progress of reaction was continuously monitored by TLC. After the completion of the reaction, the crude mixture was purified by flash column chromatography to produce an expected product (eluent: gradient mixture of EtOAc/petroleum ether). The disappearance characteristic signals of starting materials and appearance characteristic peaks of products were conveniently surveyed by ^{1}H NMR spectroscopy.

1. 2,2'-(phenylmethylene)bis(1,3,5-trimethoxybenzene)[i]

Crystalline colorless solid, mp: 192-193 ^{o}C (decomposed to black); ^{1}H NMR ($CDCl_3$) 3.49 (s, 12H), 3.78 (s, 6H), 6.10 (s, 4H), 6.21 (s, 1H), 7.03-7.16 (m, 5H) (See Supporting Information 2, Fig. S2-1).

2. 2,2'-(*p*-tolylmethylene)bis(1,3,5-trimethoxybenzene)[ii]

Off-white solid, mp: 133-134 ^{o}C (decomposed to black); ^{1}H NMR (400 MHz, $CDCl_3$) δ 2.44 (s, 3H), 3.50 (s, 6H), 3.77 (s, 12H), 6.10 (s, 4H), 6.94-6.96 (d, 2H), 7.32-7.34 (d, 2H) (See Supporting Information 2, Fig. S2-2).

3. 2,2'-((4-methoxyphenyl)methylene)bis(1,3,5-trimethoxybenzene)[iii]

White solid, mp: 133-134 °C (decomposed to black); ^{1}H NMR (400 MHz, $CDCl_3$) δ 3.50 (s, 3H), 3.76 (s, 12H), 3.78 (s, 6H), 6.10 (s, 4H), 6.16 (s, 1H), 7.03-7.04 (d, 2H), 7.17-7.19 (d, 2H) (See Supporting Information 2, Fig. S2-3).

4. 2,2'-((4-nitrophenyl)methylene)bis(1,3,5-trimethoxybenzene)[i]

Light yellow solid, mp: 156-158 °C (decomposed to black); ^{1}H NMR (400 MHz, $CDCl_3$) δ 3.44 (s, 12H), 3.71 (s, 6H), 6.02 (s, 4H), 6.18 (s, 1H), 7.07-7.09 (d, 2H), 7.92-7.94 (d, 2H) (See Supporting Information 2, Fig. S2-4).

5. 3,3'-(phenylmethylene)bis(1*H*-indole)[iii]

Reddish brown solid, mp: 138-139 °C (decomposed to black); ^{1}H NMR (400 MHz, DMSO) δ 5.83 (s, 1H), 6.83-6.88 (m, 4H), 7.02-7.06 (d, 2H), 7.15-7.19 (m, 1H), 7.25-7.29 (m, 4H), 7.34-7.38 (m, 4H), 10.82 (s, 2H) (See Supporting Information 2, Fig. S2-5).

6. 3,3'-(*p*-tolylmethylene)bis(1*H*-indole)[iv]

Blood red solid, mp: 102–103 °C (decomposed to black); ^{1}H-NMR (400 MHz, $CDCl_3$): δ 2.30 (s, 3H), 5.83 (s, 1H), 6.93 (s, 2H), 6.96-7.39 (m, 12H), 10.93 (s, 2H) (See Supporting Information 2, Fig. S2-6).

7. 3,3'-((4-Methoxylphenyl)methylene)bis(1*H*-indole)[v]

Pink solid, mp: 189-190 °C (decomposed to black); ^{1}H NMR (400 MHz, DMSO) δ 3.94 (s, 3H), 6.06 (s, 1H), 6.79-7.60 (m, 14H), 10.82 (s, 2H) (See Supporting Information 2, Fig. S2-7).

8. 3,3'-((4-nitrophenyl)methylene)bis(1*H*-indole)[vi]

Red solid, mp: 219–221 °C (decomposed to black); ^{1}H-NMR (400 MHz, DMSO): δ 6.03 (s, 1H), 6.86-6.90 (m, 4H), 7.03-7.07 (t, 2H), 7.28-7.30 (d, 2H), 7.36-7.38 (d, 2H), 7.60-7.62 (d, 2H), 8.13-8.16 (d, 2H), 10.93 (s, 2H) (See Supporting Information 2, Fig. S2-8).

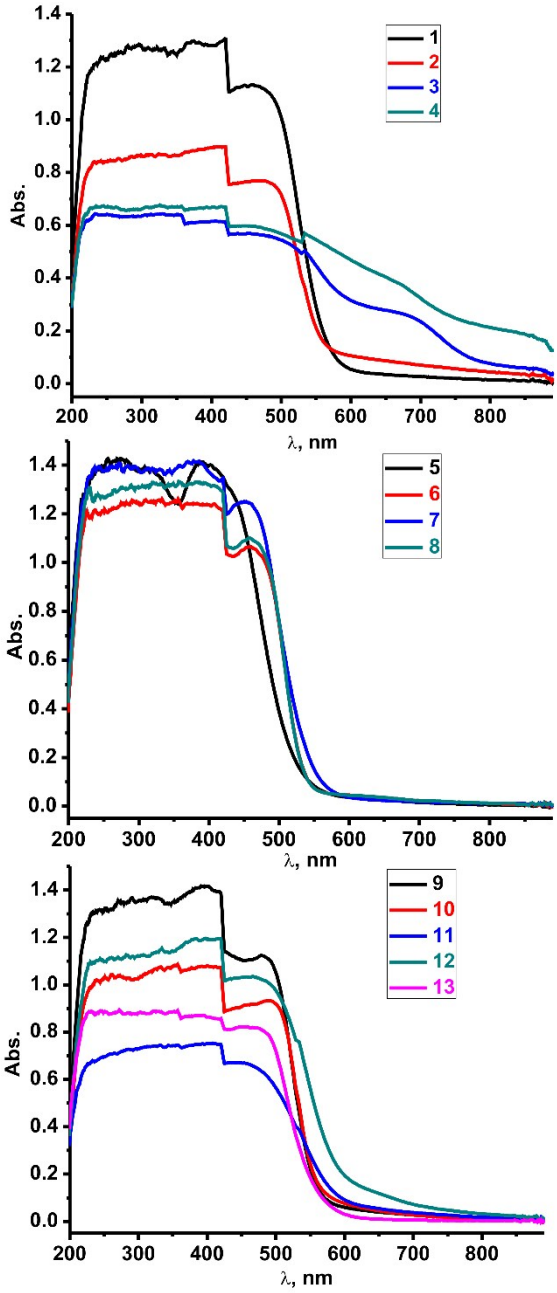

Fig. S44. Solid state UV-vis spectra of complexes **1**-**13** at 25 °C.

Table S1. Structural parameters of compounds **1**-**6**.

	1	**2**	**3**	**4**	**5**	**6**	**7**
Empirical formula	$C_{39}H_{48}N_{12}O_{47}Bi_7S_{19}F_{39}$	$C_{23}H_{32}BiF_9N_8O_{11}S_3Se_4$	$C_{29}H_{40}N_8O_9F_9S_7Bi$	$C_{29}H_{40}N_8O_9F_9S_3Se_4Bi$	$C_{54}H_{73}N_{24}Bi_4S_{12}Cl_{12}$	$C_{18}H_{24}N_8S_4Br_6Bi_2$	$C_{18}H_{24}N_8Se_4Cl_6Bi_2$
Formula weight	6408.07	1388.56	1249.12	1436.69	2704.49	1378.09	1286.86
Temperature (K)	150	150	150	150	293	293	293
Crystal system	Trigonal	triclinic	Monoclinic	Monoclinic	Monoclinic	Monoclinic	monoclinic
Space group	*R-3c*	*Pī*	$P2_1/n$	$P2_1/n$	*C2/c*	$P2_1/c$	*C2/m*
a/Å	30.7421(7)	9.0767(5)	15.1033(3)	15.3075(6)	27.2866(11)	9.393(2)	14.559(5)
b/Å	30.7421(7)	15.2872(8)	13.2707(3)	13.2282(6)	27.1101(6)	17.461(2)	12.466(3)
c/Å	70.888(2)	16.4710(7)	22.9733(4)	23.4812(9)	29.9547(11)	11.491(2)	12.369(4)
α/°	90	71.308(4)	90	90	90	90	90
β/°	90	86.504(4)	94.6380(16)	94.758(4)	117.194(5)	113.29(3)	113.06(4)
γ/°	120	82.217(4)	90	90	90	90	90
Volume ($Å^3$)	58019(2)	2144.61(19)	4589.50(14)	4738.4(3)	19709.5(15)	1731.0(7)	2065.6(13)
Z	12	2	4	4	8	2	2
ρ_{calc}/mg mm^{-3}	2.2006	2.1501	1.8076	2.0138	1.8227	2.6438	2.0688
Absorption coefficient (μ/mm^{-1})	20.189	14.222	11.358	12.868	19.514	30.304	24.306
F(000)	36339.3	1316.3	2474.7	2744.6	10314.2	1238.1	1145.5
Reflections collected	42164	16544	17863	20296	21580	3383	6258
R_{int}	0.0549	0.0483	0.0305	0.0477	0.0341	0.0284	0.1240
Data/restraints /parameters	12404/0/823	8065/0/538	8727/0/575	8961/0/576	14572/0/967	2520/0/173	2031/0/92
GOF on F^2	1.046	1.041	1.004	1.033	1.022	0.996	1.979
R_1 ($I>2б(I)$)	0.0391	0.0493	0.0344	0.0361	0.0457	0.0439	0.2839
wR_2 ($I>2б(I)$)	0.0918	0.1285	0.0939	0.1106	0.1126	0.1054	0.5764
R_1 values (all data)	0.0498	0.0549	0.0363	0.0473	0.0775	0.0575	0.3720
R_2 values (all data)	0.0975	0.1350	0.0960	0.1358	0.1377	0.1192	0.6593

Table S2. Structural parameters of compounds **7**-**13**.

	8	**9**	**10**	**11**	**12**	**13**	**14**	**15**

Empirical formula	$C_{18}H_{24}N_4Bi_2Se_4Br_6$	$C_{28}H_{43}N_9S_4Cl_6Bi_2$	$C_{28}H_{43}Bi_2Br_6N_9S_4$	$C_{28}H_{43}N_9Cl_6Se_4Bi_2$	$C_{28}H_{43}N_9Se_4Bi_2Br_6$	$C_{30}H_{46}Bi_4Br_{12}N_{10}Se_4$	$C_{31}H_{40}NO_8$	$C_{23}H_{17}N_3O_2$
Formula weight	1563.65	1261.63	1528.34	1449.20	1715.91	2657.37	512.58	367.41
Temperature (K)	293	293	293	293	293	150	293	293
Crystal system	monoclinic	tetragonal	tetragonal	tetragonal	tetragonal	monoclinic	triclinic	monoclinic
Space group	$P2_1/n$	$P4_2/ncm$	$P4_2/ncm$	$P4_2/ncm$	$P4_2/ncm$	$P2_1/c$	$P\bar{1}$	$I2/a$
a/Å	9.549(2)	19.00307(17)	19.2248(3)	19.04444(18)	19.2323(2)	12.54238(19)	8.0626(4)	17.2917(6)
b/Å	17.6588(8)	19.00307(17)	19.2248(3)	19.04444(18)	19.2323(2)	21.6905(3)	12.3582(8)	10.6763(4)
c/Å	17.763(5)	12.04528(15)	12.2798(3)	12.15557(19)	12.4100(2)	12.37785(18)	13.8011(9)	39.6733(15)
α/°	90	90	90	90	90	90	91.927(5)	90
β/°	143.57(6)	90	90	90	90	107.2678(16)	99.512(5)	91.757(4)
γ/°	90	90	90	90	90	90	101.537(5)	90
Volume (Å^3)	1779(2)	4349.75 (8)	4538.55 (15)	4408.71 (9)	4590.22 (11)	3215.62(8)	1325.66(14)	7320.7(5)
Z	4	4	4	4	4	2	2	16
ρ_{calc}/mg mm^{-3}	2.8778	1.9264	2.2366	2.1832	2.4828	2.7443	1.2840	1.3333
Absorption coefficient (μ/mm^{-1})	31.974	21.151	23.211	22.875	24.877	32.666	0.776	0.087
F(000)	1325.1	2401.6	2808.7	2671.6	3078.6	2320.0	547.9	3073.4
Reflections collected	3330	9430	11356	9141	9414	14054	8480	21069
R_{int}	0.0645	0.0381	0.0543	0.0334	0.0370	0.0442	0.0170	0.0525
Data/restraints /parameters	2477/0/173	2182/0/125	2269/0/124	2201/0/125	2291/0/125	6092/0/279	5015/0/341	8475/0/505
GOF on F^2	3.110	1.014	1.015	1.013	0.994	0.979	1.081	1.055
R_1 (I>2σ(I))	0.2524	0.0347	0.0432	0.0297	0.0288	0.0478	0.0610	0.0776
wR_2 (I>2σ(I))	0.5931	0.0897	0.1234	0.0761	0.0707	0.1268	0.1799	0.2182
R_1 values (all data)	0.3176	0.0437	0.0516	0.0336	0.0342	0.0566	0.0713	0.1578

R_2 values (all data)	0.6659	0.0973	0.1351	0.0795	0.0746	0.1371	0.1964	0.2932

[i] V. Nair, K. G. Abhilash and N. Vidya., *Org. Lett*., 2005, **7**, 5857-5859.
[ii] B. M. Babu, P. B. Thakur, N. N. Rao, G. S. Kumar and H. M. Meshram., *Tet. Lett*. 2014, **55**, 1868–1872.
[iii] P. Thirupathi and S. S. Kim., *J. Org. Chem*. 2010, **75**, 5240–5249.
[iv] P. Thirupathi and S. S. Kim., *J. Org. Chem*. 2009, **74**, 7755–7761.
[v] E. L. Armstrong, H. K. Grover and M. A. Kerr., *J. Org. Chem*. 2013, **78**, 10534−10540.
[vi] A. Z. Halimehjani, S. E. Hooshmand and E. V. Shamiri., *RSC Adv*., 2015, **5**, 21772–21777.